Royal College of Surgeons in Ireland

repository@rcsi.com

An efficient, non-viral dendritic vector for gene delivery in tissue engineering.

AUTHOR(S)

David P. Walsh, Andreas Heise, Fergal O'Brien, Sally-Ann Cryan

CITATION

Walsh, David P.; Heise, Andreas; O'Brien, Fergal; Cryan, Sally-Ann (2017): An efficient, non-viral dendritic vector for gene delivery in tissue engineering.. Royal College of Surgeons in Ireland. Journal contribution. https://hdl.handle.net/10779/rcsi.10764677.v2

HANDLE

10779/rcsi.10764677.v2

LICENCE

CC BY-NC-SA 4.0

This work is made available under the above open licence by RCSI and has been printed from https://repository.rcsi.com. For more information please contact repository@rcsi.com

URL

https://repository.rcsi.com/articles/journal_contribution/An_efficient_non-viral_dendritic_vector_for_gene_delivery_in_tissue_engineering_/10764677/2

ACCEPTED ARTICLE PREVIEW

Accepted Article Preview: Published ahead of advance online publication



An efficient, non-viral dendritic vector for gene delivery in tissue engineering

D P Walsh, A Heise, F J O'Brien, S-A Cryan

Cite this article as: D P Walsh, A Heise, F J O'Brien, S-A Cryan, An efficient, non-viral dendritic vector for gene delivery in tissue engineering, *Gene Therapy* accepted article preview 19 July 2017; doi: 10.1038/gt.2017.58.

This is a PDF file of an unedited peer-reviewed manuscript that has been accepted for publication. NPG are providing this early version of the manuscript as a service to our customers. The manuscript will undergo copyediting, typesetting and a proof review before it is published in its final form. Please note that during the production process errors may be discovered which could affect the content, and all legal disclaimers apply.

Accepted manuscript

Received 14 December 2016; revised 25 May 2017; accepted 16 June 2017; Accepted article preview online 19 July 2017

© 2017 Macmillan Publishers Limited. All rights reserved.

ACCEPTED ARTICLE PREVIEW

An Efficient, Non-Viral Dendritic Vector for Gene Delivery in Tissue Engineering

David P. Walsh[1-4], Andreas Heise[5,6], Fergal J.O'Brien[2-5], Sally-Ann Cryan[1-3,5].*

[1]*School of Pharmacy, RCSI, Dublin, Ireland*

[2]*Tissue Engineering Research Group, Department of Anatomy, RCSI, Dublin, Ireland*

[3]*Trinity Centre for Bioengineering, Trinity College Dublin, Dublin, Ireland*

[4]*Advanced Materials and Bioengineering Research (AMBER) Centre, RCSI & TCD*

[5]*Centre for Research in Medical Devices (CURAM), RCSI, Dublin and National University of Ireland, Galway, Ireland*

[6]*Pharmaceutical and Medicinal Chemistry, RCSI, Dublin, Ireland*

*Corresponding Author:

Professor Sally-Ann Cryan

School of Pharmacy,

Royal College of Surgeons in Ireland,

1st Floor, Ardilaun House (Block B), Dublin 2, Ireland

Tel: 00353-(0)1-4022741

Email: scryan@rcsi.ie

Accepted manuscript

Conflict of Interest Statement:

The authors declare no conflict of interest

Key Words:

Gene activated, Superfect, DNA delivery, Nanoparticle, Collagen Scaffold, Mesenchymal Stem Cells

Word Count: 7923

© 2017 Macmillan Publishers Limited. All rights reserved.

ACCEPTED ARTICLE PREVIEW

Abstract:

Recent developments within the field of tissue engineering (TE) have shown that biomaterial scaffold systems can be augmented via the incorporation of gene therapeutics. The objective of this study was to assess the potential of the activated polyamidoamine dendrimer (dPAMAM) transfection reagent (Superfect^{TM}) as a gene delivery system to mesenchymal stem cells (MSCs) in both monolayer and 3D culture on collagen based scaffolds. dPAMAM-pDNA polyplexes at a mass ratio (M:R) 10:1 (dPAMAM : pDNA) (1ug pDNA) were capable of facilitating prolonged reporter gene expression in monolayer MSCs which was superior to that facilitated using polyethylenimine (PEI)-pDNA polyplexes (2ug pDNA). When dPAMAM-pDNA polyplexes (1ug pDNA) were soak loaded onto a collagen-chondroitin sulphate (CCS) scaffold prolonged transgene expression was facilitated which was higher than that obtained for a PEI-pDNA polyplex (2ug pDNA) loaded scaffold. Transgene expression was dependent on the composite nature of the collagen scaffold with varying expression profiles obtained from a suite of collagen constructs including a collagen alone, collagen-CCS, collagen-hydroxyapatite, collagen-nanohydroxyapatite and collagen-hyaluronic acid scaffold. Therefore, the dPAMAM vector described herein represents a biocompatible, effective gene delivery vector for TE applications which, via matching with a particular composite scaffold type can be tailored for regeneration of various tissue defects.

Accepted manuscript

© 2017 Macmillan Publishers Limited. All rights reserved.

1. Introduction:

Significant injury or trauma can often result in irrevocable damage to bodily tissues, with treatment largely confined to the transplantation of tissue from a healthy site to the defect area in the form of an autograph or allograph. Associated clinical limitations such as the development of donor site morbidities and the consistent risk of disease transmission have encouraged the development of tissue engineering (TE) strategies which aim to regenerate, rather than replace damaged tissues via the creation of therapeutically augmented, surgically implantable constructs (1). It is widely accepted that augmenting TE constructs with growth factors can function to further enhance the regenerative capacity of the system (2). Medtronic's INFUSE bone graft, a commercial TE construct which delivers recombinant human bone morphogenetic protein-2 (rhBMP-2) on a collagen based sponge during spinal fusion procedures is associated with numerous drawbacks such as the large supraphysiological doses of rhBMP-2 protein required (3). While the delivery of a therapeutic protein directly from a scaffold system in an effective, safe manner is feasible via the use of controlled delivery systems such as micro-particles or hydrogels (4), the incorporation of therapeutic gene cargos such as plasmid DNA (pDNA) encoding particular growth factors is hypothesized to be more advantageous as it exposes the host to lower levels of the therapeutic agent, facilitating spatio-temporal controlled release of the gene at the disease site and thus potential prolonged transgene expression with reduced toxicity (5). However, the uptake of naked plasmid DNA encoding therapeutic proteins into cells is an extremely inefficient process and thus the creation of a "gene activated scaffold" system relies heavily on the field of vector assisted gene therapy. Viral systems are perhaps the most efficient mechanism of delivering exogenous nucleic acid to cells (6), however they are plagued by a large number of manufacturing and safety concerns (7). Non-viral systems have thus far been widely adopted in the scientific research field due to their ease of manufacture and minimal safety concerns (8).

Gene activated scaffolds were first conceptualized as constructs which could facilitate the *in-vivo* transfection of host cells as they migrate throughout the scaffold system (9). The principal cell type targeted for TE applications is mesenchymal stem cells (MSCs), an undifferentiated multipotent stem cell source which possess both high proliferative and self-renewal capacities as well as differentiation potential into different tissues of the mesoderm following the application of biological queues (10). Collagen scaffolds have been previously utilized in a range of TE applications such as the regeneration of burnt skin, conjunctival tissue and to induce peripheral nerve repair (11-13). Indeed within our laboratory we have developed a range of collagen based scaffolds which are amenable to multiple tissue regeneration applications .These include the use of collagen-chondroitin sulphate (collagen-CCS) (14), collagen-hyaluronic acid (CHyA) (15), collagen hydroxyapatite (collagen-HA) (16) and collagen-nanohydroxyapatite (collagen-nHA) (17) scaffolds which can be applied to numerous TE applications including bone (18), cartilage (19), cardiac (20) respiratory (21), skin (22), corneal and peripheral nerve regeneration. Numerous non-viral vectors have been assessed for the delivery of nucleic acids from these 3D scaffolds including polyethyleneimine (PEI) (23), chitosan (24) and nano-hydroxyapatite (nHA) (25). While promising levels of transgene expression have been achieved with these vectors to date, none are without their limitations, for example, PEI possesses a

© 2017 Macmillan Publishers Limited. All rights reserved.

Accepted manuscript

ACCEPTED ARTICLE PREVIEW

well-documented toxicity profile (26) while nHA has a low transfection efficiency thereby hindering its more broad use in TE, outside of that of osteogenic applications (25). Herein, we outline the potential of a different class of non-viral vector, dendrimeric polymers which are commonly used non-viral systems as monolayer transfection reagents (27), for their application in TE.

A dendrimer is a nano-sized, symmetrical molecule which possess a well-defined, homogenous architecture consisting of tree-like arms or branches radiating from a central core (28). To date, dendrimers have received relatively little interest from the field of TE, with limited reports on their transfection capability in 3D (29). One of the most widely used dendrimer families is that of the Poly (amidoamine) (PAMAM) dendrimers. The development of an "activation" process during which the mass of the dendrimer is reduced results in the formation of an "activated dendrimer" (30) with reports of up to a 50 fold magnitude increase in transfection capability (27). Realisation of this potential is illustrated in the commercialisation of a G6 activated PAMAM dendrimer (dPAMAM) as Superfect™ Transfection Reagent (Qiagen Ltd.) which is capable of facilitating transgene expression in the presence of serum and was notably utilized to deliver a 60Mb artificial mammalian chromosome into murine and hamster cells (31). Indeed the efficiency at which Superfect™ facilitates nucleic acid delivery into cells has been established in a number of studies covering a range of cell types (32-34). However, relatively few literature articles are available on the application of Superfect™ for MSC transfection (35), one of the principal cell types used in TE, or in the formation of a gene activated scaffold system for TE (36).

The objective of this study was thus to further explore the potential of the dendritic architecture in the field of TE using the commercially available dPAMAM Superfect™ reagent and determine how varying the composite nature of a collagen scaffold can influence transgene expression. Using a series of reporter gene cargos, *Gaussia Luciferase* plasmid (pGLuc*)* & green fluorescent protein plasmid (pGFP) the transfection capability of the dPAMAM structure in MSCs was confirmed. Transgene expression facilitated by various manufacturer recommended mass ratios (M:R) was assessed in 2D and comparatively analysed against a non-viral system widely used in TE, polyethyleneimine (PEI), which we have previously optimised in our laboratory for delivery of pDNA to MSCs in both 2D and 3D (23) as were the effects of treatment with dPAMAM-pDNA polyplexes on MSC cell viability. Finally, dPAMAM-pDNA polyplexes were incorporated into a suite of composite collagen based scaffolds developed within our laboratory including collagen-CCS, collagen-HyA, collagen-HA and collagen- collagen-nHA scaffolds which have demonstrated potential in numerous TE applications.

Accepted manuscript

© 2017 Macmillan Publishers Limited. All rights reserved.

Results:

Physicochemical characterisation of dPAMAM-pGLuc polyplexes

To confirm the ability of the dPAMAM reagent to condense pDNA and thus its suitability as a transfection reagent, polyplex size (nm) and concentration/ml were determined using nanoparticle tracking analysis (NTA) (Fig. 1A and 1C) for all three dPAMAM-pGLuc Mass Ratios (M:Rs) (2:1, 5:1 & 10:1 Superfect ; pDNA). NTA demonstrated that all three dPAMAM-pGLuc M:Rs are capable of forming nano-sized polyplexes which are below the target 200nm threshold to facilitate MSC transfection . A dPAMAM-pGLuc M:R 10:1 resulted in the smallest diameter polyplexes with an average size of 133.1 ± 5.7nm, however this was not statistically different to that of the dPAMAM-pGLuc M:R 2:1 (150.8 ± 9.3nm) or M:R 5:1 (138.8 ± 12.8nm) formulations. This size range was further confirmed using transmission electron microscopy (Fig. 1D (i-iii)) which indicated the presence of well defined, <200nm, spherical polyplexes in all three dPAMAM-pGLuc formulations. Furthermore, we confirmed a consistent cationic charge on formed polyplexes which was >18mV for all three dPAMAM-pGLuc M:Rs (Fig 1B). The determination of polyplex concentration is an important consideration as it may have ultimate influence on numerous properties of the formulation such as toxicity, transfection efficiency and stability. In this regard, a dPAMAM-pGLuc M:R 10:1 resulted in a statistically higher number of polyplexes/ml ($5.91x10^9 \pm 2x10^7$ polyplexes/ml) compared to that of the M:R 2:1 ($2.79x10^9 \pm 9.85x10^8$) ($p<0.01$) and M:R 5:1 ($3.35x10^9 \pm 9.8x10^8$) ($p<0.05$) formulations.

Effect of Mass Ratio (M:R) of dPAMAM-pGLuc polyplexes on monolayer MSC transgene expression

To date, relatively little work has assessed the transfection capability of dPAMAM-pDNA polyplexes in MSCs. Therefore, we investigated the effect that varying the mass ratio had on MSC transgene expression in order to ascertain the optimal formulation for use in TE applications. In this regard, the dPAMAM-pDNA M:R was found to have a significant effect on the transgene expression profile facilitated in MSCs when pGLuc was utilised as a reporter plasmid. Figure 2A demonstrates that a dPAMAM-pGLuc M:R 10:1 resulted in statistically higher levels of luciferase production compared to a dPAMAM-pGLuc M:R 2:1 & 5:1 at days 7 ($p<0.001$), 10 ($p<0.001$) and 14 ($p<0.01$) with a peak at day 7 ($6.4x10^6 \pm 2.1 x10^6$ RLUs). Both the dPAMAM-pGLuc M:R 2:1 & 5:1 both resulted in peak expression at the later time-point of day 14 with respective values of $2.5x10^6 \pm 3.3x10^5$ and $3.1x10^6 \pm 6.7x10^5$ RLUs.

Comparative analysis of dPAMAM-pGLuc M:R 10:1 (1ug pGLuc) & PEI-pGLuc N/P 7 (2ug pGLuc) transgene expression in monolayer MSCs

In this study, the pGLuc transgene expression profile facilitated by the optimal dPAMAM-pGLuc M:R 10:1 (1ug pGLuc) formulation was assessed over the longer time span of 21 days whilst also comparatively analysing it against an optimised PEI-pGLuc N/P7 (2ug pGLuc) formulation. The results illustrated in Fig. 2B have been normalised to delivered pGLuc dose (dPAMAM-1ug pGLuc, PEI-2ug pGLuc). dPAMAM-pGLuc M:R 10:1 (1ug pGLuc) resulted in a statistically higher level of transgene expression compared to PEI-pGLuc N/P7 (2ug pGLuc) at days 7, 10 & 14 ($p<0.001$). Both vectors were

© 2017 Macmillan Publishers Limited. All rights reserved.

ACCEPTED ARTICLE PREVIEW

capable of facilitating a prolonged transgene expression profile up to day 21 which peaked at day 7 with values of $6.4x10^6 \pm 2.1 x10^6$ RLUs and $3.3x10^6 \pm 6.3 x10^5$ RLUs for dPAMAM-pGLuc M:R 10:1 and PEI-pGLuc N/P 7 polyplexes respectively.

Comparative analysis of dPAMAM-pGFP M:R 10:1 (1ug pGFP) and PEI-pGFP N/P 7 (2ug pGFP) transfection efficiency in monolayer MSCs

While determination of luciferase production enables assessment of the transgene expression profile of non-viral vectors, the use of green fluorescent protein plasmid DNA (pGFP) allows for the definitive quantification of the number of MSCs transfected. In this regard, when normalised to delivered pGFP dose (Fig. 3A) there was no statistical difference found between the dPAMAM-pGFP M:R 10:1 (1ug pGFP) and PEI-pGFP N/P 7 (2ug pGFP) formulations, despite an increased dose delivered in the case of the PEI-pGFP formulation. Both PEI-pGFP and dPAMAM-pGFP obtained peak transfection efficiency at day 7 with pGFP (ug) normalised levels of 22.93 ± 1.2% and 20.8 ± 3.0% respectively. By day 14 the percentage transfection efficiency had reduced in both formulations to 3.83 ± 0.2% (PEI-pGFP N/P 7 2ug pGFP) and 4.16 ± 0.1% (dPAMAM-pGFP M:R 10:1 1ug pGFP). Visual confirmation of successfully transfected cells producing green fluorescent protein is illustrated in Fig. 3B (i) for PEI-pGFP N/P 7 2ug pGFP and Fig. 3B (ii) for dPAMAM-pGFP M:R 10:1 1ug pGFP. Overall, the dPAMAM-pDNA formulations assessed (both pGLuc & pGFP) resulted in more efficient transgene expression at a lower pDNA dose compared to that of the PEI-pDNA formulations (pGLuc & pGFP).

Assessment of the effects of dPAMAM-pDNA polyplex treatment on MSC viability

The dPAMAM structure is known to possess a degree of cytoxicity which is highly dependent on the cell type utilised (37). To date, little work has been carried out on its potential cytotoxic effects in MSCs. As such, MSCs were treated with the dPAMAM pGLuc M:R 10:1 (1ug pGLuc) formulation and cell metabolic activity quantified using an MTT assay at 24, 72 & 168 hours post-treatment (Fig. 4A). Comparative analysis was performed against PEI-pGLuc N/P 7 (2ug pGLuc) polyplexes with results expressed as a percentage of the metabolic activity of untreated MSCs. Overall, the dPAMAM-pGLuc formulation resulted in a greater percentage MSC metabolic health compared to treatment with PEI-pGLuc at all three time-points ($p<0.001$). Initial metabolic activity of MSCs treated with the dPAMAM-pGLuc formulation was 69.64 ± 3.6% which increased to 71.29 ± 2.7% by 168 hours. The PEI-pGLuc treated MSCs had a significantly reduced metabolic activity determined to be 35.63 ± 7.6% at 24 hours which further decreased to 19.09 ± 11.9% by 168 hours. The enhanced metabolic activity of MSCs treated with the dPAMAM-pGLuc M:R 10:1 formulation compared to the PEI-pGLuc N/P 7 formulation is visually evident in Fig. 4B with a clear reduction in the number of formazan crystals present (indicating lower metabolic activity) in the PEI-pGLuc treated wells (Fig. 4B (iii)) compared to the untreated control (Fig. 4B (i)) and the dPAMAM-pGLuc treated well (Fig. 4B (ii)).

Effect of dPAMAM-pGLuc mass ratio (M:R) on 3D pGLuc transgene expression from a collagen-chondroitin sulphate scaffold

As varying the dPAMAM-pGLuc M:R had an effect on transgene expression in MSC monolayer culture, the ability of all three dPAMAM-pGLuc M:Rs of 2:1, 5:1 & 10:1 to facilitate pGLuc transgene expression from a collagen-CCS scaffold was assessed when formulated using 1ug pGLuc. All three formulations were capable of facilitating transient pGLuc expression from the CCS scaffold over the 14 day period (Fig. 5A). The dPAMAM-pGLuc M:R 2:1 formulation resulted in the lowest levels of

© 2017 Macmillan Publishers Limited. All rights reserved.

Accepted manuscript

ACCEPTED ARTICLE PREVIEW

transgene expression which peaked at day 7 at $8.2x10^3 \pm 3.7x10^3$ RLUs, further falling to $2.9x10^3 \pm 2.0x10^3$ RLUs by day 14. The dPAMAM-pGLuc M:R 5:1 formulation facilitated a higher level of pGLuc transgene expression which peaked at day 3 at $3.6x10^4 \pm 1.1x10^4$ RLUs, falling to $7.2x10^3 \pm 2.1x10^3$ RLUs by day 14. In agreement with results observed in monolayer culture, a dPAMAM-pGLuc M:R 10:1 (1ug pGLuc) formulation resulted in statistically higher levels of luciferase production than both M:R 2:1 & 5:1 polyplex systems at days 3, 7 & 10 ($p<0.001$). The highest levels of pGLuc expression by dPAMAM-pGLuc M:R 10:1 was facilitated on day 3 at $8.8x10^4 \pm 3.5x10^4$ RLUs which reduced to $2.1x10^4 \pm 6.8x10^3$ RLUs by day 14.

For comparative purposes, the pGLuc transgene expression capability of the lead formulation of dPAMAM-pGLuc M:R 10:1 (1ug pGLuc) was assessed against that of an optimised PEI-pGLuc N/P10 (2ug pGLuc) formulation (23) (Fig. 5B) using a collagen-CCS scaffold. Data has been normalised to the pGLuc dose delivered. Despite the reduction in the delivered pGLuc dose within the dPAMAM-pGLuc formulation, it facilitated statistically higher levels of luciferase production compared to that of PEI-pGLuc on all of days 3, 7, 10, 14 ($p<0.001$), 21 & 28 ($p<0.05$). In this instance, the peak expression level of dPAMAM-pGLuc M:R 10:1 (1ug pGLuc) increased to $2.1 \times 10^5 \pm 3.5x10^4$ RLUs at day 3 which may reflect a slight variation in MSC response compared to the previous experiment on the effect of M:R on 3D pGLuc expression. In both the dPAMAM-pGLuc and PEI-pGLuc gene activated scaffolds a transient transgene expression profile was obtained, however the dPAMAM-pGLuc gene activated scaffold provided a more sustained profile, with consistent luciferase expression maintained from days 3-10 in the region of $2x10^5$ RLUs, while PEI suffers a rapid decrease in luciferase production from day 7 onwards. Indeed at day 28, the dPAMAM-pGLuc M:R 10:1(1ug pGLuc) formulation facilitated a pGLuc expression of $7.2x10^4 \pm 2.1x10^4$ RLUs compared to that of PEI-pGLuc N/P10 (2ug pGLuc) which resulted in a pGLuc expression of $8.8x10^3 \pm 4.0x10^3$ RLUs.

Assessment of the metabolic and proliferative health of MSCs seeded onto dPAMAM-pGLuc Collagen-CCS scaffolds

The ability of a gene activated scaffold to facilitate the transfection of host MSCs holds great promise for the healing of multiple tissue defects. Such a construct requires prompt cell infiltration, matrix formation and vascularisation once inserted *in-vivo* to ensure maximal tissue regeneration. An MTS assay was utilised to assess the metabolic activity of MSCs seeded on a CCS gene activated scaffold which was loaded with one of dPAMAM-pGLuc M:R 2:1, 5:1 or 10:1 (1ug pGLuc) as well as PEI-pGLuc N/P 10 (2ug pDNA) at 24, 72 & 168 hours post seeding (Fig. 6 (A)). In this regard, a significant decrease in the metabolic activity of each scaffold system, either dPAMAM-pGLuc (M:R 2:1, M:R 5:1 or M:R 10:1) or PEI-pGLuc N/P10 was not evident compared to the untreated control group (100% metabolic activity). All dPAMAM-pGLuc gene activated scaffolds suffered from a reduction in MSC metabolic activity at the 72 hour time point which was most pronounced for the dPAMAM-pGLuc M:R 10:1 (1ug) formulation which had an initial metabolic activity of 94.70% ± 7.3% at 24 hours which fell to 83.31% ± 10.7% by 72 hours before recovering to 93.29% ± 12.3% metabolic activity by 168 hours. This trend for a recovery of MSC metabolic activity was evident in all dPAMAM-pGLuc gene activated scaffolds by the 168 hour time point. The PEI-pGLuc N/P10 (2ug pGLuc) gene activated scaffold followed a similar trend with a reduction in the metabolic activity from 108.25% ± 3.0% at 24 hours to 96.44% ± 4.9% at 72 hours followed by a recovery to 102.72% ± 3.3% by 168 hours. Taken together these results suggest that the formation of a gene activated scaffold does not affect the metabolic health of MSCs when compared against a non-gene activated scaffold system.

Accepted manuscript

© 2017 Macmillan Publishers Limited. All rights reserved.

ACCEPTED ARTICLE PREVIEW

The effect that incorporation of dPAMAM-pGLuc polyplexes of M:R 10:1 (1ug pGLuc) into a collagen-CCS scaffold had on MSC cell proliferation was assessed via quantification of dsDNA present following 24, 72 and 168 hours post seeding (Fig. 6B). Comparative analysis was performed using PEI-pGLuc N/P 7 (2ug pGLuc) polyplexes. MSCs seeded onto a non-gene activated control scaffold display a typical proliferation profile whereby the concentration of DNA present per scaffold increases over time from 152.4 ± 28.8 ng/scaffold at 24 hours to 187.4 ± 7 ng/scaffold at 168 hours. Similar to the MTS assay, there was no observable decrease in dsDNA in either of the PEI-pGLuc or dPAMAM-pGLuc gene activated scaffolds with quantification levels of dsDNA of 183 ± 28.8 ng/scaffold and 181.3 ± 46.2 ng/scaffold respectively at 168 hours post seeding.

Live/Dead imaging allows for differential visualisation of subpopulations of live (green) and dead (red) MSCs seeded onto the dPAMAM-pGLuc M:R 10:1 (1ug pGLuc) collagen-CCS scaffold. At 72 hours post seeding (Fig. 6C (i)) the majority of live MSCs appear at the periphery of the scaffold structure with relatively few dead cells visible. However, by 168 hours (Fig. 6C (ii)) the surface of the scaffold appears covered in live MSCs whilst still retaining a relatively reduced number of dead cells thereby confirming that the structure can support MSC adherence and proliferation. Confocal microscopy (Fig. 6C (iii)) was utilised to confirm the ingress of MSCs into the scaffold structure with a majority of live MSCs displaying a typical morphology of cell spreading below the top surface of the scaffold at 168 hours post seeding.

Assessment of transgene expression from MSCs seeded on a range of dPAMAM-pGLuc gene activated collagen scaffolds

It is well documented that the specific composition of collagen based scaffolds can affect the transgene expression profile of incorporated polyplexes due to interactions between the charged polyplexes and the individual constituents within the collagen/composite materials (23, 24). In this regard, the dPAMAM-pGLuc M:R 10:1 formulation (1ug pGLuc) was soak loaded onto five different collagen based scaffolds and subsequent pGLuc transgene expression determined (Fig. 7). Similar to the above experiments, the collagen-CCS scaffold resulted in the highest levels of gene expression, peaking at day 3 with an RLU of $3.8x10^5 \pm 8.0x10^4$, slightly higher than was determined in Fig.5B, again indicating potential variation in the transfection of MSCs in 3D. The RLU level facilitated on the gene activated collagen-CCS scaffold was statistically increased over all other scaffolds at days 3, 7, & 10 ($p<0.001$). This superior transgene expression profile was maintained to the later time points of day 10-14 as previously observed. From day 21 transgene expression from the collagen-CCS scaffold was statistically lower than the collagen-HyA and collagen alone scaffold ($p<0.001$). All other gene activated scaffolds resulted in a lower level of pGLuc transgene expression in the region of $1x10^5$ RLUs from day 3 onwards.

Accepted manuscript

© 2017 Macmillan Publishers Limited. All rights reserved.

Discussion

Gene activated scaffolds for TE applications remain hindered by the lack of safe and effective gene delivery systems with current widely used non-viral vectors such as polyethylenimine (PEI) plagued by toxicity concerns . The overall objective of this study was to assess the potential of dendrimeric polymers as non-viral gene transfection vectors in the design of gene activated scaffolds for TE applications using an activated polyamidoamine dendrimer (dPAMAM) commercially available as Superfect^{TM}. Specifically, the ability of the dPAMAM vector to condense pDNA and efficiently transfect MSCs in 2D monolayer culture without prolonged toxicity effects was confirmed before an optimised formulation was soak loaded onto various collagen scaffolds to create a suite of gene expression systems with varying transgene profiles potentially applicable to a range of therapeutic TE applications.

To date, a multitude of gene activated scaffolds for TE have been described such as those incorporating PEI in both modified and unmodified forms (38, 39), chitosan (24), poly-L-lysine (40), nano-hydroxyapatite (41), cationic dextrans (42) and lipid based systems (43) to name but a few. An extensive review of current research in this area has previously been described (44). Despite the fact that greater than 20 years of research exists confirming the suitability of dendrimers for gene delivery, the architecture remains relatively overlooked by the field of TE with limited reports on their use within a 3D environment (45, 46). Indeed one of the few reports into its use is that of *Holladay* et al. whom identified that activated dPAMAM-pDNA polyplexes could result in an elongated expression profile from a collagen based matrix thereby identifying significant advantages of the architecture over other non-viral systems (29).

PAMAM dendrimers enter cells via endocytosis (47) and thus, to facilitate maximum uptake the dPAMAM-pDNA polyplexes should be cationically charged and possess a size range <200nm (48). All three manufacturer recommended mass ratios (M:R) of M:R 2:1, 5:1 & 10:1 resulted in the formation of nano-sized cationic polyplexes when used to complex pDNA, with M:R 10:1 achieving the smallest size of 133.1 ± 5.7nm (Fig. 1A) and a cationic potential of 18.3 ± 2.1mV (Fig 1B). This size range is smaller than values reported in the literature for dPAMAM-pDNA particles such as 500-1660nm (37), however many of these reports predate the use of the more sensitive NTA technique. The dPAMAM-pDNA M:R 10:1 formulation resulted in the generation of the highest number of polyplexes ($5.9x10^9 \pm 2x10^7$ per ml) compared to the 2:1 ($p<0.01$) and 5:1 ($p<0.05$) formulations (Fig. 1C). While there is little published data on the "optimal" concentration of polyplex solution for the efficient transfection of cells, this data at the very least suggests an increased probability of association between the dPAMAM-pDNA M:R 10:1 formulation and the cell membrane due to a fundamental increase in the number of polyplexes present, however it could also potentially increase the toxicity of the system. TEM was utilised to further confirm relative size distribution and spherical morphology of the polyplexes (Fig. 1D (i-iii)) whereby discrete sub <200nm polyplexes were visible using all three M:Rs.

Holladay et al. have previously demonstrated that a dPAMAM-pGLuc M:R 2:1 is optimal in MSCs, achieving an RLU value of approximately $2.5x10^3$ after 24 hours when a dose of 0.5ug pGLuc was

© 2017 Macmillan Publishers Limited. All rights reserved.

Accepted manuscript

delivered. Other groups have utilised the dPAMAM reagent at higher M:R values to achieve superior transfection in multiple cell types including both primary cells and cell lines such as M:R 9:1 (49), M:R 12:1 (50) and M:R 30:1 (51). Here, we demonstrate in Fig. 2A that of all three dPAMAM-pGLuc M:Rs examined, M:R 10:1 resulted in the highest levels of pGLuc expression, peaking at day 7 with $6.4x10^6$ ± $2.1x10^6$ RLUs. In direct comparison to a PEI-pGLuc N/P 7 formulation complexed with 2ug pGLuc which our laboratory has previously optimised for delivery to MSCs (23), we illustrate superior transgene expression when the dPAMAM-pGLuc M:R 10:1 is utilised complexed with half the pGLuc dose (Fig. 2B). Within the literature conflicting reports exist on which of the two aforementioned vectors are superior with reports both of the superiority of the dPAMAM structure (52) and that of PEI (53). Admittedly however, direct comparisons with other studies can be difficult unless thorough control of experimental parameters such as cell passage and seeding density are accounted for.

Figure 3A and 3B illustrates the transfection efficiency and representative fluorescence images when dPAMAM-pGFP M:R 10:1 (1ug pGFP) and PEI-pGFP N/P7 (2ug pGFP) polyplexes were utilised to transfect MSCs. In this instance, when normalised to the dose of pGFP delivered (1ug for dPAMAM-pGFP and 2ug for PEI-pGFP) comparable levels of transfection efficiency between the two non-viral systems was obtained. PEI-pGFP (2ug pGFP) resulted in a peak level of transfection of 22.93% at day 7, a finding in agreement with our previous work (24) while the dPAMAM-pGFP (1ug pGFP) formulation caused peak transfection efficiency of 20.8% at day 7. Others have demonstrated dPAMAM-pGFP transfection efficiencies of between 8% and 35% depending on the cell type used and mass ratio, with the trend that higher mass ratios upwards of 45:1 achieved maximum transfection in human aortic smooth muscle cells (37). Nevertheless there is a clear dichotomy between the pGLuc reporter system (where the dPAMAM-pGLuc polyplex resulted in a significant enhancement in transgene expression over the PEI-pGLuc polyplex system) and the pGFP reporter system (where both dPAMAM-pGFP and PEI-pGFP have comparable percentage transfection efficiencies), a finding which should be borne in mind if only one of the two reporter systems is reported upon.

The toxicity of PAMAM dendrimers is an important consideration in their development as TE vectors due to previous reports of increased platelet aggregation (54), induction of autophagy (55) and apoptotic cell death (56). Toxicity remains hugely dependent on the cell type utilised with studies illustrating that dPAMAM-pDNA M:R 10:1 can result in effectively 0% cell viability of human aorta endothelial cells while the same formulation retains ~50-60% viability in smooth muscle cells (37). To determine the potential cytotoxic effects of transfecting MSCs in monolayer culture with dPAMAM-pDNA polyplexes we utilised a colorimetric MTT assay. Herein we have demonstrated that treating MSCs with the highest dPAMAM-pDNA M:R investigated, M:R 10:1 resulted in an initial reduction in MSC metabolic activity to 69.64 ± 3.6% at 24 hours which was maintained by day 7 at 71.2 ± 2.6% (Fig.4A). A reduction to ~70% metabolic health in MSCs following treatment with PAMAM dendrimers has previously been reported, however this was for a G5 dendrimer formulated at a nitrogen : phosphate (N/P ratio) of 8-10 therefore making a direct comparison difficult (57). Furthermore, we confirmed the multitude of documented reports of both the acute and prolonged toxicity effects of PEI-pDNA polyplexes (26) which had an initial 24 hour MSC metabolic activity of 35.6 ± 7.6% which reduced to 19.09 ± 11.9% by day 7. These results are visually observable in Fig. 4B (i-iii) whereby a reduction in the number of formazan crystals indicates reduced metabolic activity of MSCs. It can be speculated that the toxicity of these systems can be extrapolated to their polymeric structure as PEI is inherently non-degradable due to its amine-carbon backbone and thus may accumulate within cells while the PAMAM dendrimer consists mainly of amide bonds and thus is

© 2017 Macmillan Publishers Limited. All rights reserved.

Accepted manuscript

ACCEPTED ARTICLE PREVIEW

comparatively more degradable (58). Indeed we are just beginning to understand the biological consequences of using such nano sized drug delivery systems (59) with reports that the dPAMAM vector can interfere with cell signalling cascades involved in cell growth, differentiation, survival and apoptosis (60). That said, it has been suggested that the judicious, informed development of dendrimer chemistry for a specific biomedical applications can alleviate such concerns (61), an approach worth considering in future explorations of this architecture.

Since the seminal work on gene activated scaffolds (9), there have been numerous reports of the creation of gene activated collagen scaffolds including PEI mediated delivery of bone morphogenetic protein 4 (pBMP4), pBMP2 and pVEGF (62, 63), calcium phosphate-pBMP-2 (64) and liposomal-pBMP-2 (65) to name a few. Indeed within our group we have extensive experience working with a range of gene activated systems for multiple tissue engineering applications including PEI (23) , chitosan (24) and nHA based non-viral systems (41). Initial success aside it is important to acknowledge that each vector to date possesses certain limitations such as chitosan being more effective in cartilage TE (unpublished data).The field lacks a versatile non-viral system which can be applied to multiple TE applications while still achieving superior tissue regeneration compared to a scaffold alone approach. Therefore, we initially assessed the ability of the three dPAMAM-pDNA M:Rs utilised in 2D, namely M:R 2:1, 5:1 & 10:1 (all 1ug pDNA) to facilitate pGLuc transgene expression on a collagen-CCS scaffold system (Fig. 5A). In agreement with the monolayer transfection data, the dPAMAM-pGLuc M:R 10:1 (1ug pGLuc) formulation resulted in the highest levels of transgene expression which was statistically higher than dPAMAM-pGLuc M:R 2:1 and M:R 5:1 at days 3, 7, & 10 ($p<0.001$) with a peak value of $8.8x10^4 \pm 3.5x10^4$ RLUs at day 3. No statistically significant increases in pGLuc transgene expression were observed when the dPAMAM vector was utilised to deliver higher pGLuc doses of 2ug or 5ug (Supplementary Figure 1). While there is a tendency towards increased transgene expression with the higher pGLuc dose of 5ug this leads to increased variability in the levels of luciferase expression. Importantly, the levels of transgene expression obtained when using the lower 1ug pGLuc dose in this manuscript is comparable to that observed with other vector-pGLuc formulations we have successfully utilised both *in-vitro* and *in-vivo* such as chitosan and PEI (23, 24, 63). The inclusion of such higher pGLuc doses also necessitates a large increase in the amount of dPAMAM vector incorporated within each scaffold which itself could lead to associated side effects such as toxicity

Figure 5B illustrates a comparative analysis of this dPAMAM-pGLuc M:R 10:1 (1ug pGLuc) gene activated scaffold against our previously optimised PEI-pGLuc N/P 10 (2ug pGLuc) gene activated scaffold (23). Here we demonstrate the superiority of the dendrimeric architecture over the non-viral vector PEI in achieving efficient 3D transfection of MSCs. The dPAMAM-pGLuc polyplex formulation resulted in prolonged transgene expression up to 28 days with a peak expression of $2.1x10^5$ RLUs compared to that of the PEI-pGLuc formulation of $9.0x10^4$ RLUs. Expression was higher for the dPAMAM-pGLuc gene activated scaffold at all days 3, 7, 10, 14 ($p<0.001$) 21 & 28 ($p<0.05$). The pGLuc expression profile illustrated here is similar to that obtained by *Holladay et al*. whom showed prolonged expression up to day 14 in a dPAMAM-pGLuc collagen matrix achieving an RLU of $2.5x10^5$ albeit with a lower seeding density of 10,000 cells per scaffold (29). The cause for the difference in the transgene expression levels obtained in 3D between the dPAMAM & PEI vectors is likely due to the interaction of the respective polyplex formulations with the composite collagen scaffold which in this case contains a negatively charged chondroitin sulphate component. We suggest, as has been previously hypothesised by others (66) that the cationic charge present on PEI-pDNA and dPAMAM-pDNA polyplex formulations may, due to electrostatic interactions with the

© 2017 Macmillan Publishers Limited. All rights reserved.

ACCEPTED ARTICLE PREVIEW

components of the composite collagen scaffold sequester the polyplexes to varying degrees within the construct. In any case, use of the dPAMAM-pDNA polyplex system results in a prolonged transgene expression profile from the 3D construct, a prized characteristic in the TE field. This is most likely due to both the electrostatic interactions mentioned above but also the migratory activities of MSCs as they move throughout the structure, becoming transfected over time as opposed to a bolus transfection as would occur in 2D monolayer transfection.

The collagen based scaffolds used in these experiments possess the dual advantage of being both biocompatible and biodegradable and as such, toxicity of the system will depend largely on MSC interaction with dPAMAM-pDNA polyplexes within the 3D environment. We hypothesised that due to the increased surface area available throughout the porous scaffold structure the potential for toxicity of dPAMAM-pDNA formulations would be reduced due to a decrease in immediate contact between MSCs and dPAMAM-pDNA polyplexes. In agreement with this hypothesis, Fig. 6 (A) illustrates the percentage MSC metabolic activity obtained using an MTS assay when all three dPAMAM-pDNA M:Rs were utilised to form a gene activated system on a collagen-CCS scaffold. An overall trend for both the PEI-pGLuc N/P 10 (2ug pGLuc) gene activated scaffold and the various dPAMAM-pGLuc M:R 2:1, M:R 5:1 or M:R 10:1 (1ug pGLuc) gene activated scaffolds was a reduction in the metabolic activity of MSCs at 72 hours which then began to recover by the 168 hours. The results obtained here are likely caused by the inward infiltration of MSCs into the gene activated construct and thus maximal exposure to embedded polyplexes may occur at the 72 hour time point.

The biocompatible nature of these gene activated structures was further confirmed in Fig. 6 (B) whereby no statistically significant difference was observed in the concentration of DNA present per scaffold on either of a dPAMAM-pGLuc M:R 10:1 (1ug pGLuc) or PEI-pGLuc N/P 10 (2ug pGLuc) compared to an untreated, non-gene activated control scaffold at 24 hours, 72 hours and 168 hours post seeding with MSCs. To account for the detection of any loaded pGLuc DNA by the DNA quantification process the results have been normalised to DNA detected from a respective gene activated scaffold (dPAMAM-PGLuc or PEI-pGLuc) not seeded with MSCs. This result demonstrates that not only is the gene activated structure biocompatible but it also supports the attachment and proliferation of MSCs over time, a key attribute for its ultimate success in an *in-vivo* setting. Furthermore, using a combination of Live/Dead staining and confocal microscopy we confirmed full coverage of the dPAMAM-pGLuc M:R 10:1 (1ug pGLuc) collagen-CCs scaffold structure with live MSCs 168 hours post seeding (Fig. 6C (ii)) and ingress of the MSCs into the scaffold architecture without compromising cell viability (Fig 6C (iii)). MSCs displayed a typical “spreading” morphology thereby confirming that the gene activated scaffold can support MSC adherence, proliferation and metabolic health. Taken together, it appears evident that the complex 3D environment of the scaffold structure with its interconnected porous network through which MSCs can migrate and proliferate will mitigate much of the toxicity profile of non-viral transfection agents.

Finally, we incorporated the optimal dPAMAM-pDNA M:R 10:1 formulation into a range of collagen based scaffolds developed within our laboratory. These included the collagen-CCS scaffold previously utilised, a collagen alone, collagen-HyA, collagen-HA and collagen-nHA scaffolds which have potential uses in multiple TE applications encompassing bone, cartilage, nerve, skin, cardiac, corneal and respiratory tissue regeneration. In this instance, the collagen-CCS scaffold resulted in peak levels of luciferase expression at day 3 ($3.8x10^5 \pm 8.x10^4$ RLUs) which was maintained above $2x10^5$ RLUs past day 10 (Fig. 7). These values are somewhat higher than the levels predicted in Figure 5 and may reflect a combination of variation in MSC response and the complex interactions of the

© 2017 Macmillan Publishers Limited. All rights reserved.

Accepted manuscript

scaffold-polyplex-MSCs which are occurring. In all instances, all gene activated scaffolds except the collagen-HA scaffold resulted in prolonged pGLuc transgene expression, with detectable luciferase levels still present at day 28. This reduced transgene expression in the collagen-HA scaffold may be explained via hydrogen bonding occurring between the plentiful amino groups present in the fractured dendrimer structure and the hydroxyl ions on the surface of hydroxyapatite crystals thereby reducing availability of dPAMAM-pGLuc polyplexes for MSC transfection. This is a logical hypothesis when it is considered the collagen-nHA scaffold contains approximately half the %w/w hydroxyapatite compared with the collagen-HA scaffold (200%w/w in collagen-HA compared with 100%w/w in collagen-nHA) and thus the potential for hydrogen bonding is reduced with an observable increase in pGLuc transgene expression.

Overall this study has highlighted the potential of the relatively overlooked dendrimeric polymer architecture in the development of gene activated scaffolds for the TE. The dPAMAM vector is an efficient non-viral delivery vector which is capable of inducing superior transfection in a difficult to transfect cell type, namely MSCs in both 2D and 3D culture at relatively low pDNA doses. Furthermore, matching of the dPAMAM vector with a specific composite collagen scaffold facilitates temporal control over transgene expression thereby suggesting tailoring of the transgene expression profile to a particular tissue defect site is plausible. The nature and architecture of the dendrimeric class of vectors therefore possesses significant potential within the TE field for a range of applications.

© 2017 Macmillan Publishers Limited. All rights reserved.

Materials and methods:

All materials were supplied by Sigma-Aldrich, Ireland unless otherwise stated.

Plasmid propagation & purification

The reporter plasmids *Gaussia Luciferase* (pGLuc; New England Biolabs, Massachusetts, USA) and Green Fluorescent Protein (pGFP; Amaxa, Lonza, Cologne AG, Germany) were propagated via the transformation of Subcloning Efficiency™ DH5α™ chemically competent *Escherichia coli* cells (Life Technologies, Ireland). pGLuc and pGFP plasmid DNA was isolated and purified using an Endotoxin Free Maxi-prep Kit (Qiagen, UK) as per the manufacturer's instructions.

Superfect-pDNA & Polyethyleneimine-pDNA polyplex formation

Superfect (Qiagen, UK)-pDNA polyplexes were prepared as per the manufactures guidelines. Briefly, pDNA was added to sterile OptiMEM serum free media (Gibco, Ireland) followed by addition of the required volume of Superfect™ reagent. Superfect-pDNA polyplexes were formed at mass ratios of 2:1, 5:1 & 10:1 (Superfect: pDNA). In all polyplex solutions, 1ug pDNA was utilised. Following addition, the mixture was allowed to equilibrate at room temperature for approximately 5-10 minutes before use.

Branched PEI was purchased from Sigma Aldrich (Ireland) and purified via a dialysis method. For this, PEI was dissolved in deionised water and loaded into Cellu-Sep H1 membranes (25kDa MWCO). This was dialysed against a 400 fold excess of deionised water a total of four times over night before the remaining PEI was lyophilised for use. Previous optimisation within our laboratory concluded that N/P 7 (nitrogen :phosphate ratio) results in optimal transfection efficiency in 2D culture, while N/P 10 is most suitable for 3D transfection (both formulations contain 2ug pDNA) (23). Briefly, pDNA was added to sterile molecular grade water followed by dropwise addition of PEI and 30 minutes equilibration at room temperature.

Physicochemical characterisation of Superfect-pDNA polyplexes

Polyplex diameter (nm) and concentration (number of polyplexes/ml) were assessed via nanoparticle tracking analysis (NTA) utilising a Nanosight NS300 (Malvern, UK). Samples were prepared as previously described in a 50µl volume in ultrapure water before being diluted to 0.5ml for measurement following equilibration. Samples were loaded into a laser module sample chamber which allowed for temperature control at 22^0C. Real time video analysis of the polyplexes was recorded via an in-built sCMOS camera with computer controlled motorized focus. Automatic data analysis was performed on recorded data using the NTA 2.3 software. For zeta potential (mv) analsysis, polyplexes were prepared as previously descibed before being diluted to 1ml and assessed using a Malvern Zetasizer ZS 3000.

To further confirm the size of Superfect-pDNA polyplexes transmission electron microscopy was utilised. Briefly, Superfect-pGLuc poyplexes were made as previously described. A drop of polyplex suspension was placed on a silicon monoxide carbon-coated copper grid (200 mesh, Mason technologies). Samples were allowed to air dry for approximately 10-15 minutes before being stained with 2% uranyl acetate solution. Excess stain was removed using filter paper and the grids

© 2017 Macmillan Publishers Limited. All rights reserved.

allowed to air dry fully before analysis. Imaging was preformed using a Hitachi H-7650 Transmission Electron Microscope (Hitachi High Technologies, Berkshire, UK) at 120kV.

Mesenchymal stem cell isolation and expansion

Rat Mesenchymal Stem Cells (rMSCs) were isolated from flushed tibiae and femora bone marrow of Sprague-Dawley rats. Cells were cultured in T175 adherent cell flasks (Sarstedt, Germany) at an initial seeding density of $1x10^6$ cells per flask in complete culture media consisting of Dulbecco's Modified Eagles Medium (DMEM) supplemented with: 2% penicillin/streptomycin, 1% glutamax, 1% L-glutamine, 1% non-essential amino acids and 10% FBS. Flasks were maintained in an incubator at 37^0C with 5% CO_2 and 90% humidity. All experiments were performed using passage 5 rMSCs.

Demonstration of 2D transfection capability in MSCs

The reporter plasmids pGLuc & pGFP were utilized in this study to determine transgene expression profile and transfection efficiency respectively. In terms of transgene expression; approximately 24 hours prior to transfection the cells were subjected to 0.25% trypsin/EDTA, counted using a haemocytometer and seeded on 6 well Costar™ adherent plates (Fischer Scientific) at a density of $5X10^4$ cells per well. Superfect-pGLuc polyplexes at M:R 2:1, 5:1 & 10:1 (all 1ug pDNA) were formulated as previously described using OptiMEM serum free media (Gibco, Ireland) and, following equilibration diluted in DMEM fully supplemented media. PEI-pGLuc polyplexes were formulated as previously described in biological grade H_20 and subsequently diluted with OptiMEM. Approximately 500µl of transfection solution was added to each designated well in triplicate. The plates were incubated with the transfection solution for four hours at which point it was removed and each well was washed with 1 ml of PBS. 2mls of fully supplemented DMEM was then added to each well and each plate incubated at 37^0C in 5% CO_2. Samples were taken for analysis of luciferase production at days 3, 7, 10, 14 and 21 via withdrawing 1ml of complete media from each well and replacing it with 1ml of fresh media**.** Luciferase content of each sample was determined using a Pierce™ *Gaussia* Luciferase Flash Assay Kit (Thermo Scientific, Ireland) as per the manufacturer's instructions.

Cells transfected with Superfect-pGFP or PEI-pGFP were first visualised using a Leica DMIL microscope (Leica Microsystems, Switzerland) using a 488nm fluorescent filter at 7 days post transfection. The cells were then trypsinized and fixed in 5% formalin before being re-suspended in 200µl of PBS. The cell suspension was then analysed using a fluorescence activated cell sorter (FACS Canto II, BD Biosciences, UK) and GFP fluorescence expressed as a percentage of GFP positive over GFP negative cells.

Effect of Mass Ratio (M:R) of Superfect-pDNA polyplexes on MSC cell viability

The metabolic activity of rMSCs in the presence of Superfect-pDNA polyplexes was determined using a colorimetric MTT Cell Growth Assay (Merck Millipore, Ireland). Briefly, MSCs were seeded in 96 well plates at a density of 10,000 cells per well. Superfect-pGLuc polyplexes at M:R 10:1 carrying 0.2µg pGLuc were prepared as previously described. This pDNA dose was equivalent to approximately 1ug in a 6 well plate with $5x10^4$ cells. Comparative analysis was preformed against PEI (N/P 7, 0.4µg pDNA). Following transfection for four hours as described above, each well was washed with PBS and replaced with complete growth media. At 24, 72 and 168 hours post transfection 10µl of MTT reagent was added to each well. Four hours post MTT addition, produced formazan crystals were dissolved in DMSO and the absorbance was determined at 570nm with a reference wavelength of 630nm. The absorbance reading obtained from non-transfected cells functioned as a 100% viability control with cell viability expressed as a percentage of this control.

© 2017 Macmillan Publishers Limited. All rights reserved.

ACCEPTED ARTICLE PREVIEW

Five different collagen (SLB, New Zealand) based scaffolds used in this study which included collagen alone, collagen-CCS, collagen-HyA, collagen-HA and collagen-nHA scaffolds. In all instances, collagen based slurries were formed before an optimised lyophilisation technique developed by *O'Brien et al.* was applied to create the scaffold (67). The specific formation of the collagen-CCS, collagen-HyA and collagen-HA slurries have been described elsewhere (24) as has the formation of the collagen-nHA slurry (41). Scaffolds were then cross-linked dehydrothermally (DHT) at 105^0C for 24 hours in a vacuum oven (Vacucell 22; MMM, Germany) and subsequently cut into cylindrical 9.6mm sections for all experiments.

Superfect-pGLuc polyplexes were initially formulated at three different M:Rs 2:1, 5:1 & 10:1 all with 1ug pDNA while PEI was formulated at N/P10 with 2ug pDNA. Scaffolds were formed as previously described and were hydrated in PBS before being chemically cross-linked using a mixture of 6mM N-(3-dimethylaminopropyl)-N'-ethylcarbodiimide hydrochloride (EDC) and 5.5mM N-hydroxysuccinimide (NHS). Superfect-pGLuc (1ug pDNA) and PEI-pGLuc (2ug pDNA) polyplexes (both formulated as 50ul transfection solutions) were soak loaded onto the scaffolds via applying 25ul of transfection solution to one side of the scaffold. The scaffolds were allowed to equilibrate for 10 minutes before $2.5x10^5$ MSCs were added to the same side of the scaffold in approximately 25ul of OptiMEM. The scaffolds were incubated at 37^0C for 15 minutes, carefully flipped over and the additions repeated on the opposite side (25ul transfection solution followed by 25ul ($2.5x10^5$) rMSCs) such that the final dose of pGLuc per scaffold was 1ug in the case of the Superfect-pGLuc constructs and 2ug in the case of the PEI-pGLuc constructs. Approximately 2mls of complete DMEM containing 10% FBS (Superfect-gene activated scaffolds) or serum free OptiMEM (PEI-gene activated scaffolds) was added to each well. Following 24 hours at 37^0C the scaffolds were transferred to a new plate containing 1ml of complete DMEM media in all wells. At each time point of 3, 7, 10, 14, 21 & 28 approximately 500ul of supernatant was removed for analysis and replaced with fresh DMEM media. Transgene expression was determined using a Pierce™ *Gaussia* Luciferase Flash Assay Kit as per the manufacturer's instructions.

Assessment of the metabolic activity of MSCs seeded on Superfect-pGLuc & PEI-pGLuc gene activated scaffolds

The cellular viability of rMSCs seeded onto Superfect-pGLuc and PEI-pGLuc gene activated scaffolds was investigated using the surrogate markers of cell metabolic activity and DNA quantification. With regard to the former, Superfect-pGLuc polyplexes at M:R 10:1 (1ug pGLuc) and PEI-pGLuc polyplexes at N/P 10 (2ug pGLuc) were formulated as previously described and soak loaded onto collagen-CCS scaffolds. Following 3D MSC transfection as previously described, scaffolds were incubated at 37^0C for the required time of 24, 72 or 168 hours. At each time-point scaffolds were transferred into an empty well of a 24 well tissue culture plate and a 4:1 media: MTS (CellTiter 96® AQ_{ueous} One Solution Cell Proliferation Assay System, Promega) solution was added to each well. The plate was incubated for a further three hours at 37^0C before 120ul of the solution was transferred in triplicate to a 96 well plate. The absorbance of each sample was read at 490nm and values were corrected against the background reading for media alone. Data is expressed as a percentage cell metabolic activity compared to the non-gene activated collagen-CCS scaffold. For the quantification of dsDNA rMSCs were seeded onto PEI-pGLuc or Superfect-pGLuc gene activated scaffolds as previously described above and at each time point the scaffold was transferred to 1ml of cell lysis buffer (0.2M carbonate buffer with 1% triton X). DNA was quantified using a Quant-iT™ PicoGreen® dsDNA kit (Invitrogen,

© 2017 Macmillan Publishers Limited. All rights reserved.

Accepted manuscript

ACCEPTED ARTICLE PREVIEW

UK) as per the manufacturer's instructions. The concentration of DNA present in each sample was determined against a generated standard curve and the results have been normalised to DNA detected from a respective (PEI-pGLuc (2ug pGLuc) or dPAMAM-pGLuc (1ug pGLuc) gene activated scaffold maintained under cell culture conditions but without seeding of MSCs.

Live/Dead staining of MSCs seeded on a Superfect-pGLuc M:R 10:1 gene activated scaffold

Superfect-pGLuc polyplexes at M:R 10:1 (1ug pGLuc) were formulated as previously described and soak loaded onto collagen-CCS scaffolds. Approximately 72 or 168 hours post seeding with MSCs scaffolds were submerged in 300ul Live/Dead stain (488/570nm) (Invitrogen) for approximately 20 minutes. Scaffolds were then mounted onto a cover slip, inverted and imaged immediately using an Eclipse 90i plus DS R91 microscope (Nikon, Japan). Composite scaffold images were automatically formed using NIS Elements software. For confocal imaging, scaffolds were submerged in Live/Dead stain as described and mounted onto glass slides. Imaging was performed using a Carl Zeiss 710 confocal laser scanning microscope with a Plan-Apochromat 40x/1.4 Oil DIC M27 objective lens (Fuji) coupled with Zen 2008 software.

Statistical analysis

Results are expressed as the mean $\pm$ standard deviation of three independent repeats. All samples were run in triplicate for each repeat. Statistical significance was assessed using a One-Way ANOVA followed by Bonferroni's post-hoc analysis unless otherwise stated. Significance was determined using P values of * <0.05, **<0.01 and ***<0.001.

Accepted manuscript

© 2017 Macmillan Publishers Limited. All rights reserved.

ACCEPTED ARTICLE PREVIEW

Acknowledgements

This study was undertaken as part of the Translational Research in Nanomedical Devices (TREND) research group, School of Pharmacy, RCSI, facilitated via a Science Foundation Ireland Investigators Program 13/IA/1840. The authors would like to thank Brenton Cavanagh, RCSI, Ireland, for his assistance in obtaining TEM & Live/Dead images.

Conflict of Interest Statement

The authors declare no conflict of interest

Accepted manuscript

© 2017 Macmillan Publishers Limited. All rights reserved.

ACCEPTED ARTICLE PREVIEW

Bibliography

1. Williams DF. To engineer is to create: the link between engineering and regeneration. Trends in biotechnology. 2006;24(1):4-8.
2. Richardson TP, Peters MC, Ennett AB, Mooney DJ. Polymeric system for dual growth factor delivery. Nat Biotech. 2001;19(11):1029-34.
3. Carragee EJ, Hurwitz EL, Weiner BK. A critical review of recombinant human bone morphogenetic protein-2 trials in spinal surgery: emerging safety concerns and lessons learned. The spine journal : official journal of the North American Spine Society. 2011;11(6):471-91.
4. Quinlan E, Thompson EM, Matsiko A, O'Brien FJ, Lopez-Noriega A. Long-term controlled delivery of rhBMP-2 from collagen-hydroxyapatite scaffolds for superior bone tissue regeneration. Journal of controlled release : official journal of the Controlled Release Society. 2015;207:112-9.
5. Tierney EG, Duffy GP, Cryan SA, Curtin CM, O'Brien FJ. Non-viral gene-activated matrices: next generation constructs for bone repair. Organogenesis. 2013;9(1):22-8.
6. Robbins PD, Ghivizzani SC. Viral Vectors for Gene Therapy. Pharmacology & Therapeutics. 1998;80(1):35-47.
7. Seow Y, Wood MJ. Biological Gene Delivery Vehicles: Beyond Viral Vectors. Molecular Therapy: the Journal of the American Society of Gene Therapy. 2009;17(5):767-77.
8. Glover DJ, Lipps HJ, Jans DA. Towards safe, non-viral therapeutic gene expression in humans. Nature reviews Genetics. 2005;6(4):299-310.
9. Bonadio J, Smiley E, Patil P, Goldstein S. Localized, direct plasmid gene delivery in vivo: prolonged therapy results in reproducible tissue regeneration. Nat Med. 1999;5(7):753-9.
10. Kern S, Eichler H, Stoeve J, Klüter H, Bieback K. Comparative analysis of mesenchymal stem cells from bone marrow, umbilical cord blood, or adipose tissue. Stem cells. 2006;24(5):1294-301.
11. Yannas IV. Tissue and organ regeneration in adults: Springer Science & Business Media; 2001.
12. Zhang M, Yannas I. Peripheral Nerve Regeneration. In: Yannas I, editor. Regenerative Medicine II. Advances in Biochemical Engineering. 94: Springer Berlin Heidelberg; 2005. p. 67-89.
13. Chamberlain LJ, Yannas IV, Hsu HP, Strichartz G, Spector M. Collagen-GAG substrate enhances the quality of nerve regeneration through collagen tubes up to level of autograft. Experimental neurology. 1998;154(2):315-29.
14. Murphy CM, Haugh MG, O'Brien FJ. The effect of mean pore size on cell attachment, proliferation and migration in collagen-glycosaminoglycan scaffolds for bone tissue engineering. Biomaterials. 2010;31(3):461-6.
15. Matsiko A, Levingstone TJ, O'Brien FJ, Gleeson JP. Addition of hyaluronic acid improves cellular infiltration and promotes early-stage chondrogenesis in a collagen-based scaffold for cartilage tissue engineering. Journal of the mechanical behavior of biomedical materials. 2012;11:41-52.
16. Gleeson J, Plunkett N, O'Brien F. Addition of hydroxyapatite improves stiffness, interconnectivity and osteogenic potential of a highly porous collagen-based scaffold for bone tissue regeneration. Eur Cell Mater. 2010;20:218-30.
17. Cunniffe GM, Dickson GR, Partap S, Stanton KT, O'Brien FJ. Development and characterisation of a collagen nano-hydroxyapatite composite scaffold for bone tissue engineering. Journal of materials science Materials in medicine. 2010;21(8):2293-8.

© 2017 Macmillan Publishers Limited. All rights reserved.

Accepted manuscript

ACCEPTED ARTICLE PREVIEW

18. Lyons FG, Al-Munajjed AA, Kieran SM, Toner ME, Murphy CM, Duffy GP, et al. The healing of bony defects by cell-free collagen-based scaffolds compared to stem cell-seeded tissue engineered constructs. Biomaterials. 2010;31(35):9232-43.
19. Levingstone TJ, Thompson E, Matsiko A, Schepens A, Gleeson JP, O'Brien FJ. Multi-layered collagen-based scaffolds for osteochondral defect repair in rabbits. Acta Biomater. 2016;32:149-60.
20. Brougham CM, Levingstone TJ, Jockenhoevel S, Flanagan TC, O'Brien FJ. Incorporation of fibrin into a collagen-glycosaminoglycan matrix results in a scaffold with improved mechanical properties and enhanced capacity to resist cell-mediated contraction. Acta Biomater. 2015;26:205-14.
21. O'Leary C, Cavanagh B, Unger RE, Kirkpatrick CJ, O'Dea S, O'Brien FJ, et al. The development of a tissue-engineered tracheobronchial epithelial model using a bilayered collagen-hyaluronate scaffold. Biomaterials. 2016;85:111-27.
22. O'Brien FJ, Harley BA, Yannas IV, Gibson LJ. The effect of pore size on cell adhesion in collagen-GAG scaffolds. Biomaterials. 2005;26(4):433-41.
23. Tierney EG, Duffy GP, Hibbitts AJ, Cryan S-A, O'Brien FJ. The development of non-viral gene-activated matrices for bone regeneration using polyethyleneimine (PEI) and collagen-based scaffolds. Journal of Controlled Release. 2012;158(2):304-11.
24. Raftery RM, Tierney EG, Curtin CM, Cryan SA, O'Brien FJ. Development of a gene-activated scaffold platform for tissue engineering applications using chitosan-pDNA nanoparticles on collagen-based scaffolds. Journal of controlled release : official journal of the Controlled Release Society. 2015;210:84-94.
25. Curtin CM, Cunniffe GM, Lyons FG, Bessho K, Dickson GR, Duffy GP, et al. Innovative collagen nano-hydroxyapatite scaffolds offer a highly efficient non-viral gene delivery platform for stem cell-mediated bone formation. Advanced materials (Deerfield Beach, Fla). 2012;24(6):749-54.
26. Godbey WT, Wu KK, Hirasaki GJ, Mikos AG. Improved packing of poly(ethylenimine)/DNA complexes increases transfection efficiency. Gene Ther. 1999;6(8):1380-8.
27. Dufès C, Uchegbu IF, Schätzlein AG. Dendrimers in gene delivery. Advanced Drug Delivery Reviews. 2005;57(15):2177-202.
28. Abbasi E, Aval SF, Akbarzadeh A, Milani M, Nasrabadi HT, Joo SW, et al. Dendrimers: synthesis, applications, and properties. Nanoscale Research Letters. 2014;9(1):247-.
29. Holladay C, Keeney M, Greiser U, Murphy M, O'Brien T, Pandit A. A matrix reservoir for improved control of non-viral gene delivery. Journal of controlled release : official journal of the Controlled Release Society. 2009;136(3):220-5.
30. Dennig J, Duncan E. Gene transfer into eukaryotic cells using activated polyamidoamine dendrimers. Reviews in Molecular Biotechnology. 2002;90(3–4):339-47.
31. De Jong G, Telenius A, Vanderbyl S, Meitz A, Drayer J. Efficient in-vitro transfer of a 60-Mb mammalian artificial chromosome into murine and hamster cells using cationic lipids and dendrimers. Chromosome research : an international journal on the molecular, supramolecular and evolutionary aspects of chromosome biology. 2001;9(6):475-85.
32. Maruyama-Tabata H, Harada Y, Matsumura T, Satoh E, Cui F, Iwai M, et al. Effective suicide gene therapy in vivo by EBV-based plasmid vector coupled with polyamidoamine dendrimer. Gene Ther. 2000;7(1):53-60.
33. Rudolph C, Lausier J, Naundorf S, Muller RH, Rosenecker J. In vivo gene delivery to the lung using polyethylenimine and fractured polyamidoamine dendrimers. The journal of gene medicine. 2000;2(4):269-78.
34. Mathew A, Cao H, Collin E, Wang W, Pandit A. Hyperbranched PEGmethacrylate linear pDMAEMA block copolymer as an efficient non-viral gene delivery vector. International journal of pharmaceutics. 2012;434(1-2):99-105.
35. Gheisari Y, Soleimani M, Azadmanesh K, Zeinali S. Multipotent mesenchymal stromal cells: optimization and comparison of five cationic polymer-based gene delivery methods. Cytotherapy. 2008;10(8):815-23.

Accepted manuscript

© 2017 Macmillan Publishers Limited. All rights reserved.

ACCEPTED ARTICLE PREVIEW

36. Braun CS, Vetro JA, Tomalia DA, Koe GS, Koe JG, Middaugh CR. Structure/function relationships of polyamidoamine/DNA dendrimers as gene delivery vehicles. Journal of pharmaceutical sciences. 2005;94(2):423-36.
37. Kiefer K, Clement J, Garidel P, Peschka-Süss R. Transfection Efficiency and Cytotoxicity of Nonviral Gene Transfer Reagents in Human Smooth Muscle and Endothelial Cells. Pharmaceutical research. 2004;21(6):1009-17.
38. Hosseinkhani H, Hosseinkhani M, Gabrielson NP, Pack DW, Khademhosseini A, Kobayashi H. DNA nanoparticles encapsulated in 3D tissue-engineered scaffolds enhance osteogenic differentiation of mesenchymal stem cells. Journal of biomedical materials research Part A. 2008;85(1):47-60.
39. Ow Sullivan MM, Green JJ, Przybycien TM. Development of a novel gene delivery scaffold utilizing colloidal gold-polyethylenimine conjugates for DNA condensation. Gene Ther. 2003;10(22):1882-90.
40. Capan Y, Woo BH, Gebrekidan S, Ahmed S, DeLuca PP. Preparation and Characterization of Poly (D,L-Lactide-Co-Glycolide) Microspheres for Controlled Release of Poly(L-Lysine) Complexed Plasmid DNA. Pharmaceutical research. 1999;16(4):509-13.
41. Castano IM, Curtin CM, Shaw G, Murphy JM, Duffy GP, O'Brien FJ. A novel collagen-nanohydroxyapatite microRNA-activated scaffold for tissue engineering applications capable of efficient delivery of both miR-mimics and antagomiRs to human mesenchymal stem cells. Journal of controlled release : official journal of the Controlled Release Society. 2015;200:42-51.
42. Hosseinkhani H, Azzam T, Kobayashi H, Hiraoka Y, Shimokawa H, Domb AJ, et al. Combination of 3D tissue engineered scaffold and non-viral gene carrier enhance in vitro DNA expression of mesenchymal stem cells. Biomaterials. 2006;27(23):4269-78.
43. Xie Y, Yang ST, Kniss DA. Three-dimensional cell-scaffold constructs promote efficient gene transfection: implications for cell-based gene therapy. Tissue Eng. 2001;7(5):585-98.
44. O'Rorke S, Keeney M, Pandit A. Non-viral polyplexes: Scaffold mediated delivery for gene therapy. Progress in Polymer Science. 2010;35(4):441-58.
45. Bao T, Wang H, Zhang W, Xia X, Zhou J, Weng W, et al. Application of Dendrimer/Plasmid hBMP2 complexes loaded into a B-TCP/Collagen Scaffold in the treatment of femoral rat defects Biomedical Engineering: Applications, Basis and Communications. 2014;26(01):1450005.
46. Keeney M, van den Beucken JJJP, van der Kraan PM, Jansen JA, Pandit A. The ability of a collagen/calcium phosphate scaffold to act as its own vector for gene delivery and to promote bone formation via transfection with VEGF165. Biomaterials. 2010;31(10):2893-902.
47. Kitchens KM, Foraker AB, Kolhatkar RB, Swaan PW, Ghandehari H. Endocytosis and Interaction of Poly (Amidoamine) Dendrimers with Caco-2 Cells. Pharmaceutical research. 2007;24(11):2138-45.
48. Rejman J, Oberle V, Zuhorn IS, Hoekstra D. Size-dependent internalization of particles via the pathways of clathrin- and caveolae-mediated endocytosis. The Biochemical journal. 2004;377(Pt 1):159-69.
49. Zhou D, Cutlar L, Gao Y, Wang W, O'Keeffe-Ahern J, McMahon S, et al. The transition from linear to highly branched poly(β-amino ester)s: Branching matters for gene delivery. Science Advances. 2016;2(6):e1600102.
50. Georgiou TK, Phylactou LA, Patrickios CS. Synthesis, Characterization, and Evaluation as Transfection Reagents of Ampholytic Star Copolymers: Effect of Star Architecture. Biomacromolecules. 2006;7(12):3505-12.
51. Shi S-L, Dan B, Liu F, Lin L-R, Fu Z-G, Jing G-J, et al. Synthesis and characterization of a novel cationic polymer gene delivery vector. International journal of molecular medicine. 2010;26(4):491.
52. Newland B, Zheng Y, Jin Y, Abu-Rub M, Cao H, Wang W, et al. Single Cyclized Molecule Versus Single Branched Molecule: A Simple and Efficient 3D "Knot" Polymer Structure for Nonviral Gene Delivery. Journal of the American Chemical Society. 2012;134(10):4782-9.
53. Banerjee P, Reichardt W, Weissleder R, Bogdanov A, Jr. Novel hyperbranched dendron for gene transfer in vitro and in vivo. Bioconjugate chemistry. 2004;15(5):960-8.

Accepted manuscript

© 2017 Macmillan Publishers Limited. All rights reserved.

ACCEPTED ARTICLE PREVIEW

54. Jones CF, Campbell RA, Franks Z, Gibson CC, Thiagarajan G, Vieira-de-Abreu A, et al. Cationic PAMAM dendrimers disrupt key platelet functions. Mol Pharm. 2012;9(6):1599-611.
55. Li C, Liu H, Sun Y, Wang H, Guo F, Rao S, et al. PAMAM nanoparticles promote acute lung injury by inducing autophagic cell death through the Akt-TSC2-mTOR signaling pathway. Journal of molecular cell biology. 2009;1(1):37-45.
56. Lee JH, Cha KE, Kim MS, Hong HW, Chung DJ, Ryu G, et al. Nanosized polyamidoamine (PAMAM) dendrimer-induced apoptosis mediated by mitochondrial dysfunction. Toxicology letters. 2009;190(2):202-7.
57. Santos JL, Oramas E, Pêgo AP, Granja PL, Tomás H. Osteogenic differentiation of mesenchymal stem cells using PAMAM dendrimers as gene delivery vectors. Journal of Controlled Release. 2009;134(2):141-8.
58. Choi YJ, Kang SJ, Kim YJ, Lim YB, Chung HW. Comparative studies on the genotoxicity and cytotoxicity of polymeric gene carriers polyethylenimine (PEI) and polyamidoamine (PAMAM) dendrimer in Jurkat T-cells. Drug and chemical toxicology. 2010;33(4):357-66.
59. Akhtar S. Cationic nanosystems for the delivery of small interfering ribonucleic acid therapeutics: a focus on toxicogenomics. Expert opinion on drug metabolism & toxicology. 2010;6(11):1347-62.
60. Akhtar S, Chandrasekhar B, Attur S, Yousif MHM, Benter IF. On the nanotoxicity of PAMAM dendrimers: Superfect® stimulates the EGFR–ERK1/2 signal transduction pathway via an oxidative stress-dependent mechanism in HEK 293 cells. International journal of pharmaceutics. 2013;448(1):239-46.
61. Duncan R, Izzo L. Dendrimer biocompatibility and toxicity. Adv Drug Deliv Rev. 2005;57(15):2215-37.
62. Huang YC, Simmons C, Kaigler D, Rice KG, Mooney DJ. Bone regeneration in a rat cranial defect with delivery of PEI-condensed plasmid DNA encoding for bone morphogenetic protein-4 (BMP-4). Gene Ther. 2005;12(5):418-26.
63. Curtin CM, Tierney EG, McSorley K, Cryan SA, Duffy GP, O'Brien FJ. Combinatorial gene therapy accelerates bone regeneration: non-viral dual delivery of VEGF and BMP2 in a collagen-nanohydroxyapatite scaffold. Advanced healthcare materials. 2015;4(2):223-7.
64. Endo M, Kuroda S, Kondo H, Maruoka Y, Ohya K, Kasugai S. Bone regeneration by modified gene-activated matrix: effectiveness in segmental tibial defects in rats. Tissue Eng. 2006;12(3):489-97.
65. Park J, Lutz R, Felszeghy E, Wiltfang J, Nkenke E, Neukam FW, et al. The effect on bone regeneration of a liposomal vector to deliver BMP-2 gene to bone grafts in peri-implant bone defects. Biomaterials. 2007;28(17):2772-82.
66. Hortensius RA, Becraft JR, Pack DW, Harley BA. The effect of glycosaminoglycan content on polyethylenimine-based gene delivery within three-dimensional collagen-GAG scaffolds. Biomaterials science. 2015;3(4):645-54.
67. O'Brien FJ, Harley BA, Yannas IV, Gibson L. Influence of freezing rate on pore structure in freeze-dried collagen-GAG scaffolds. Biomaterials. 2004;25(6):1077-86.

Accepted manuscript

© 2017 Macmillan Publishers Limited. All rights reserved.

Figure Legends

Figure 1: Effect of dPAMAM-pGLuc Mass Ratio (M:R) on polyplex size and concentration. Illustrated above is (A) polyplex diameter (nm) , (B) polyplex zeta potential and (C) polyplex concentration per ml of dPAMAM-pGLuc polyplexes (1ug pGLuc) at mass ratios 2:1, 5:1 & 10:1 (dPAMAM:pDNA). The polyplex size of each formulation was confirmed using (C) transmission electron microscopy (TEM) for each of dPAMAM-pGLuc M:R 2:1 (i), M:R 5:1 (ii) & M:R 10:1 (iii). All three formulations were capable of forming polyplexes potentially suitable for MSC transfection. Results are expressed as the mean ± standard deviation (n=3), **p<0.01 and *p<0.05.

Figure 2: 2D Transfection capability in MSCs using the reporter system pGLuc. (A) The dPAMAM-pGLuc M:R 10:1 formulation resulted in a statistically higher level of pGLuc transgene expression in MSCs compared to both the dPAMAM-pGLuc M:R 2:1 & 5:1 formulations at days 7 (p<0.001), 10 (p<0.001) & 14 (p<0.01). (B) In comparison to an optimised PEI-pGLuc N/P 7 (2ug pGLuc) formulation, dPAMAM-pGLuc M:R 10:1 (1ug pGLuc) resulted in statistically higher transgene expression at days 7, 10 & 14 (p<0.001). Results are expressed as the mean ± standard deviation (n=3), **p<0.01, ***p<0.001..

Figure 3: 2D Transfection capability in MSCs using the reporter system pGFP. (A) Both the PEI-pGFP N/P 7 (2ug pGFP) and dPAMAM-pGFP M:R 10:1 (1ug pGFP) resulted in a peak transfection efficiency at day 7 of 22.93 ± 1.2% and 20.8 ± 3.9% respectively. No statistical difference in transfection efficiency was found between both formulations. (B) GFP positive cells were visually observable for both formulations at day 7. Results are expressed as the mean ± standard deviation (n=3).

Figure 4: Assessment of the effects of dPAMAM-pDNA polyplex treatment on MSC viability. MSC metabolic activity (A) was quantified following treatment with dPAMAM-pDNA polyplexes. The dPAMAM-pGLuc M:R 10:1 formulation maintained a significantly higher percentage cell metabolic activity compared to PEI-pGLuc at the time points of 24, 72 & 168 hours (p<0.001). A clear reduction in the amount of formazan crystals present is apparent for PEI-pGLuc treated MSCs (B (iii)) compared to the control (B (i)) and dPAMAM-pGLuc (B (ii)) treated wells. Results are expressed as the mean ± standard deviation (n=3), **p<0.01, ***p<0.001.

Figure 5: Gene activated scaffold transgene expression profile. (A) The dPAMAM-pGLuc M:R 10:1 formulation facilitated the highest levels of pGLuc transgene expression compared to dPAMAM-pGLuc M:R 2:1 and M:R 5:1 formulations on a collagen-CCS scaffold. (B) When compared to an optimised PEI-pGLuc N/P 7 (2ug pGLuc), the dPAMAM-pGLuc M:R 10:1 (1ug pGLuc) facilitated statistically higher pGLuc expression on days 3, 7, 10, 14 (p<0.001), 21 & 28 (p<0.05) on a collagen-CCS scaffold. Results are expressed as the mean ± standard deviation (n=3), *p<0.05, ***p<0.001.

Figure 6: Effect of dPAMAM-pGLuc mass ratio (M:R) on 3D MSC metabolic activity. (A) A significant reduction in the metabolic activity of MSCs seeded onto multiple gene activated collagen-CCS scaffolds (dPAMAM-pGLuc M:R 2:1, M:R 5:1, M:R 10:1 or PEI-pGLuc N/P 10) was not evident compared that of untreated MSCs. (B) Quantification of dsDNA up to 168 hours post seeding of MSCs onto a PEI-pGLuc N/P 10 or dPAMAM-pGLuc M:R 10:1 demonstrates no significance changes in DNA content compared to a non-gene activated control scaffold. Live/Dead imaging of dPAMAM-pGLuc M:R 10:1 (1ug pGLuc) collagen-CCS scaffolds at 72 hours (C (i)) and 168 hours (C (ii)) post seeding with MSCs illustrated complete coverage of the scaffold surface by 168 hours with ingress of live cells into the scaffold structure confirmed by z-stack confocal microscopy at 168 hours (C (iii)). Results are expressed as the mean ± standard deviation (n=3).

Figure 7: Assessment of transgene expression from MSCs seeded on a range of dPAMAM-pGLuc gene activated collagen scaffolds. Illustrated above are the pGLuc transgene expression profiles obtained from a series of composite collagen scaffolds which have been “activated” with the optimal dPAMAM-pGLuc M:R 10:1 (1ug pGLuc) formulation. The highest level of transgene expression was observed for a collagen chondroitin

© 2017 Macmillan Publishers Limited. All rights reserved.

Accepted manuscript

ACCEPTED ARTICLE PREVIEW

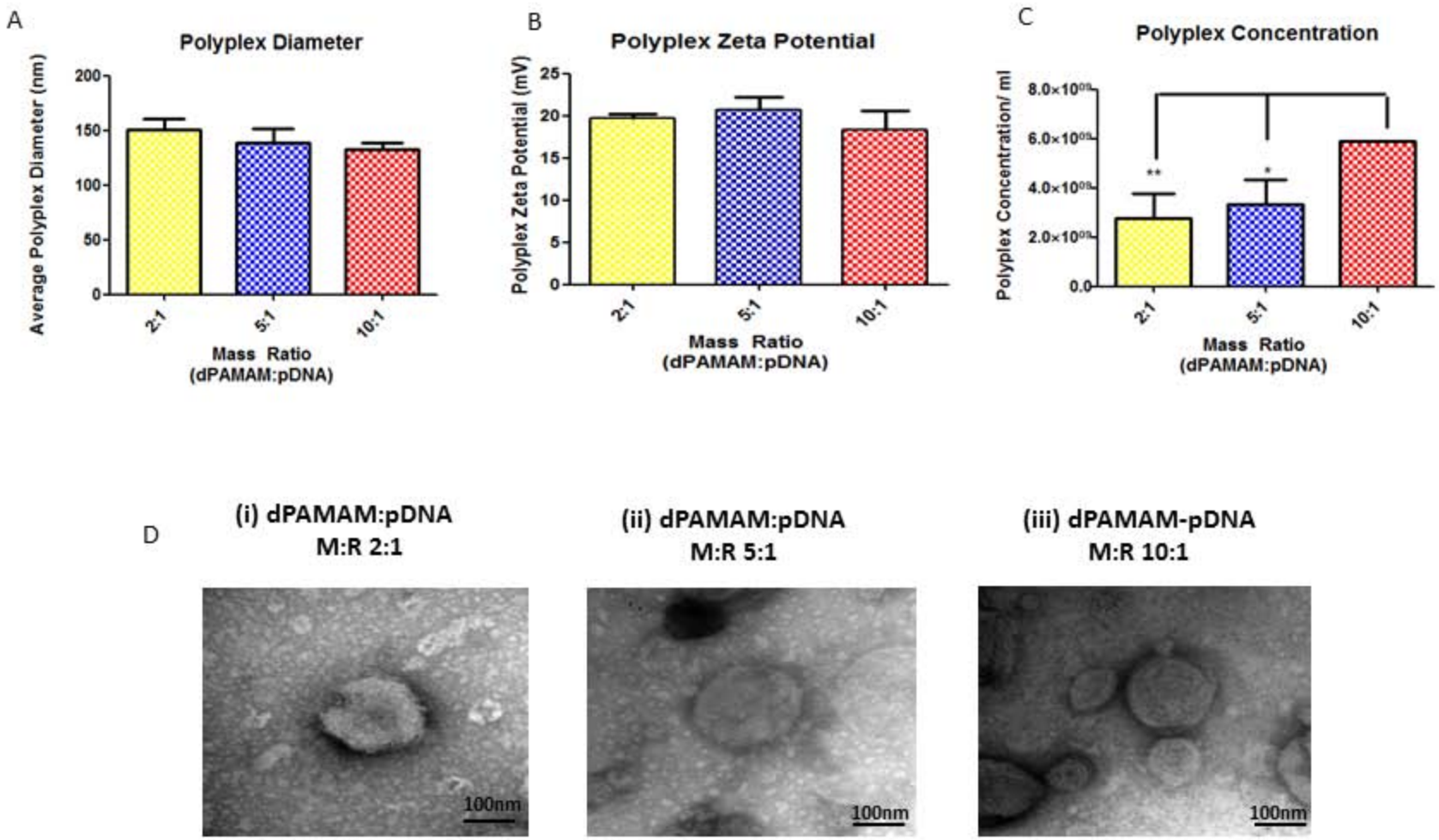
sulphate (CCS) scaffold (red) which was significantly higher than all other scaffolds at days 3-14. Results are expressed as the mean ± standard deviation (n=3) ***p<0.001.

Supplementary Figure 1: The Effect of pGLuc Dose on 3D Transgene Expression. Illustrated above is the transgene expression levels obtained when dPAMAM-pGLuc M:R 10:1 formulations were utilised to transfect MSCs on a collagen-CCS scaffold using 1ug, 2ug or 5ug pGLuc. No statistically significant increases in pGLuc transgene expression were observed when the dPAMAM vector was utilised to deliver higher pGLuc doses of 2ug or 5ug. Results are expressed as the mean ± standard deviation (n=3).

Accepted manuscript

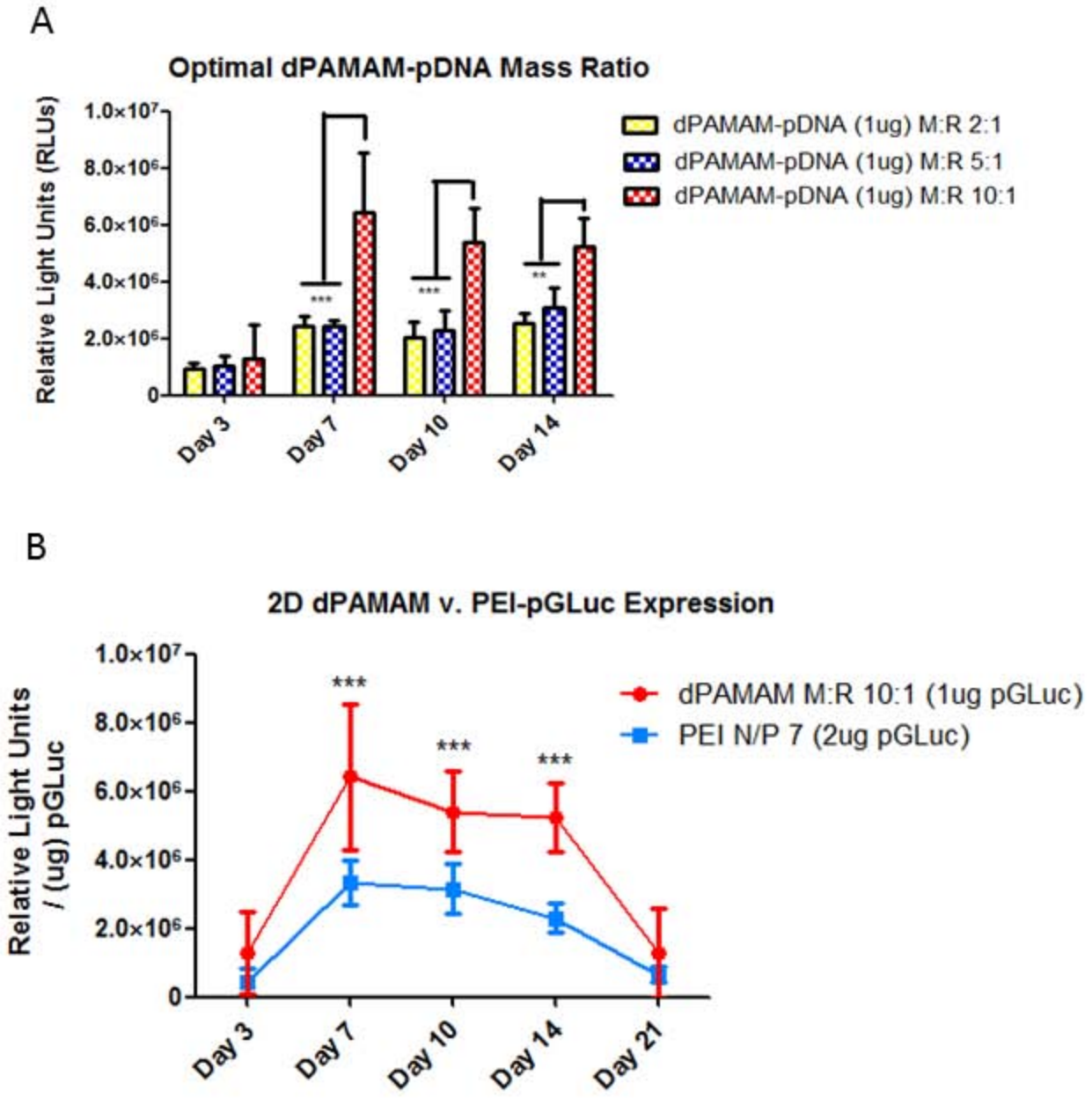
© 2017 Macmillan Publishers Limited. All rights reserved.

Figure 1:



© 2017 Macmillan Publishers Limited. All rights reserved.

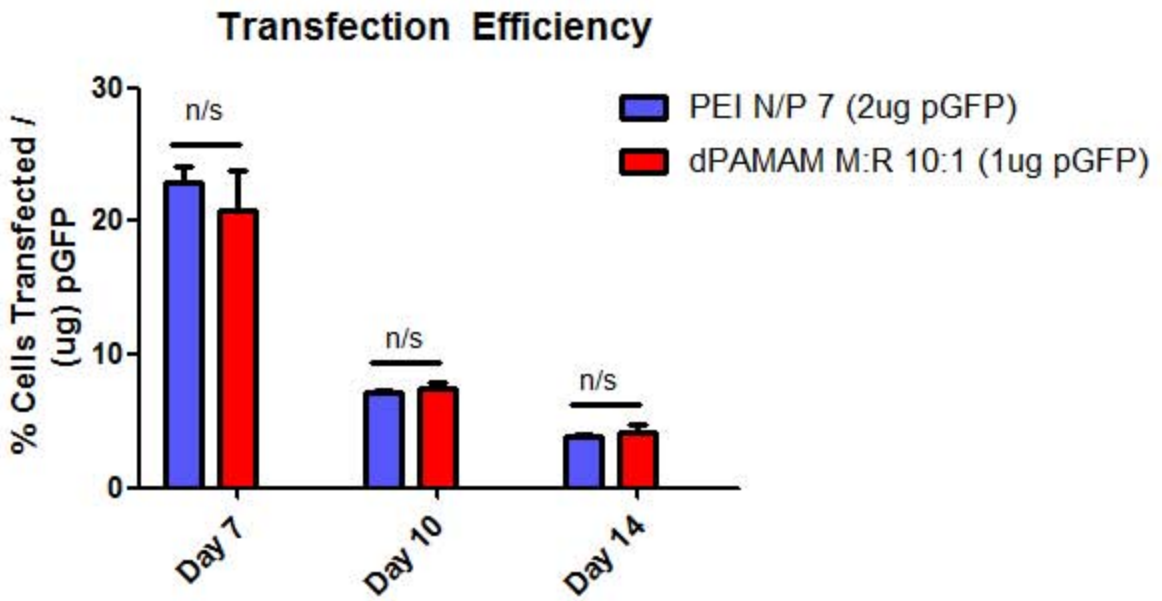
Figure 2:



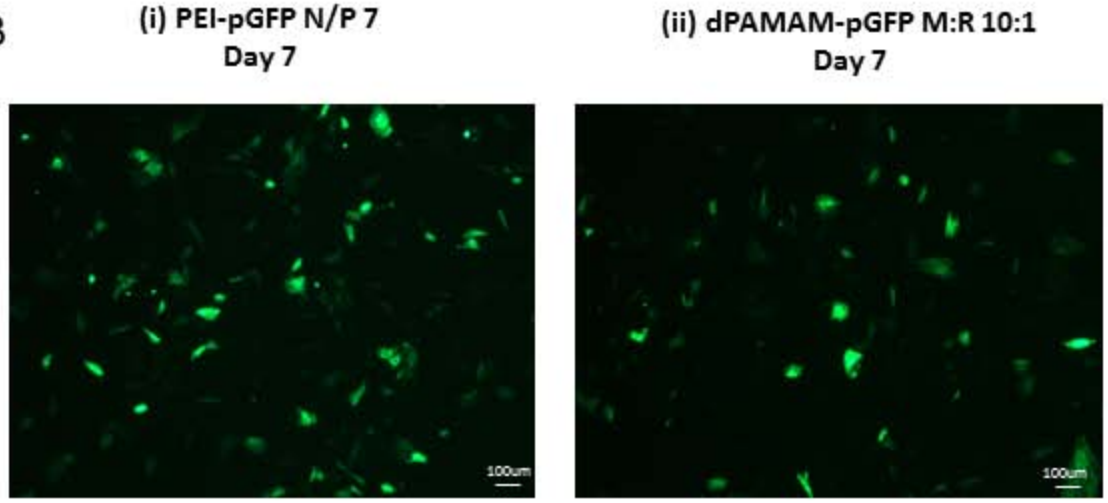
© 2017 Macmillan Publishers Limited. All rights reserved.

Figure 3:

A



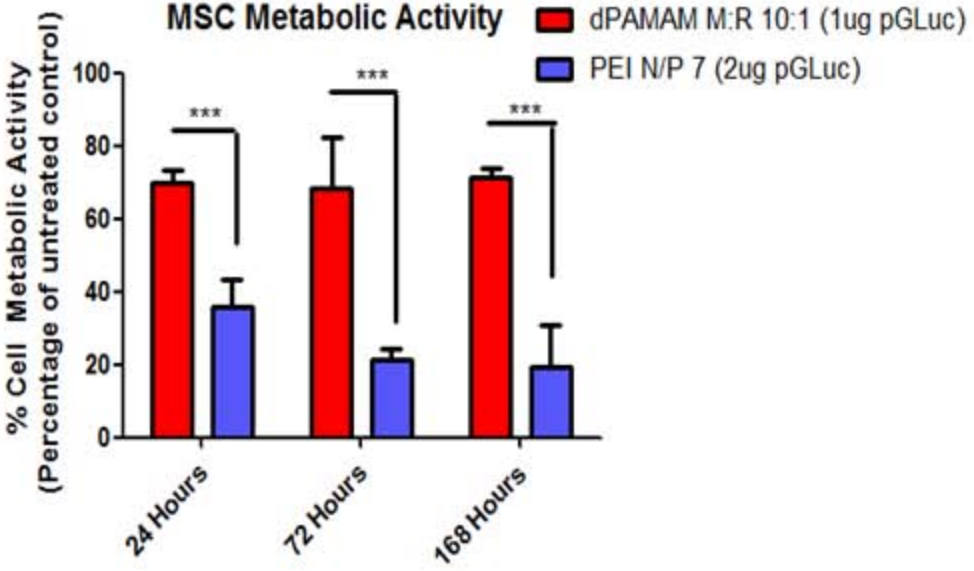
B



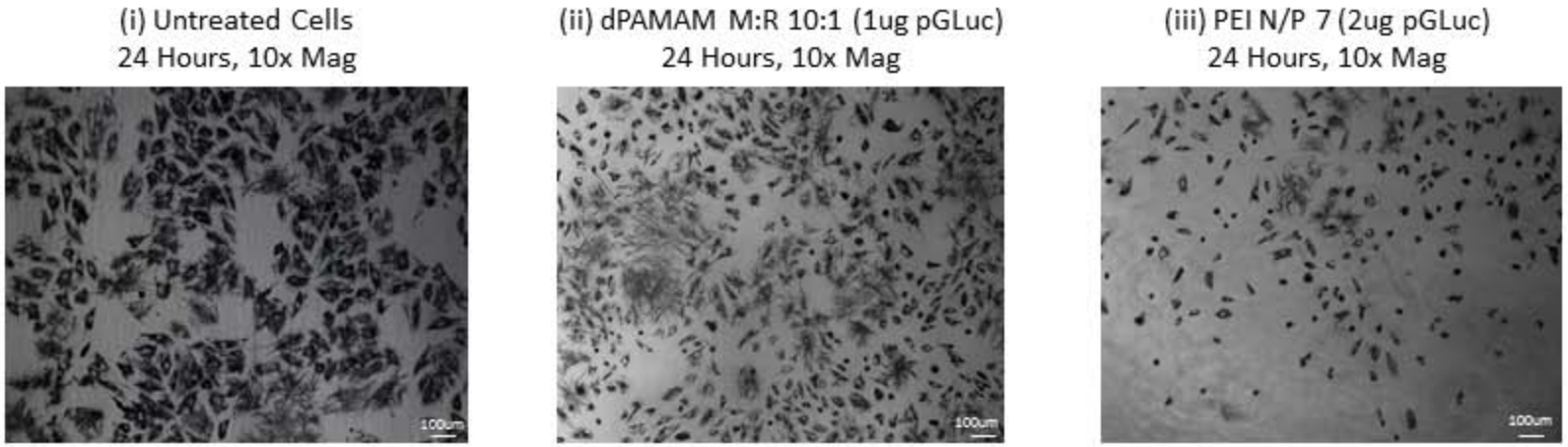
© 2017 Macmillan Publishers Limited. All rights reserved.

Figure 4:

A

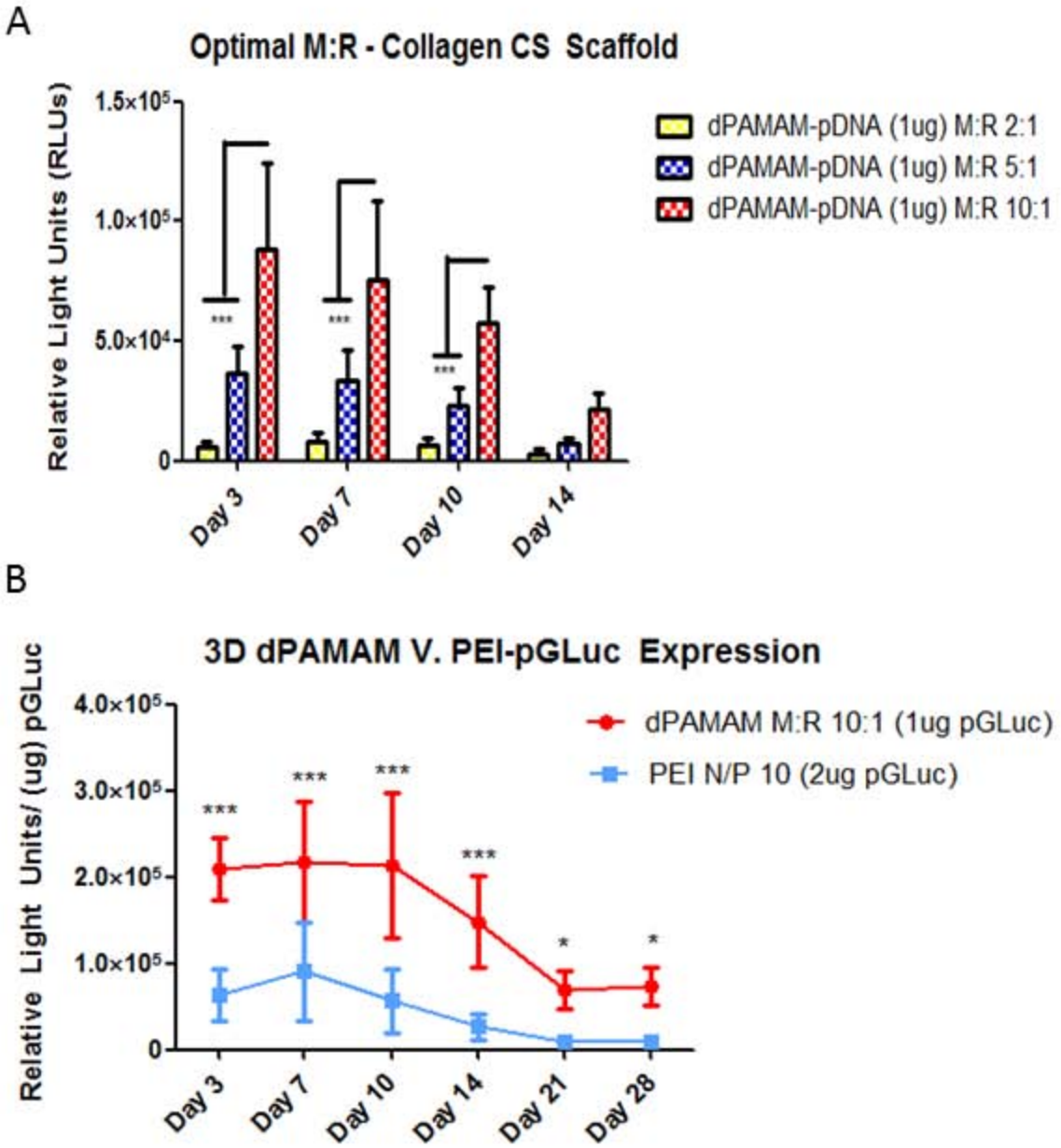


B



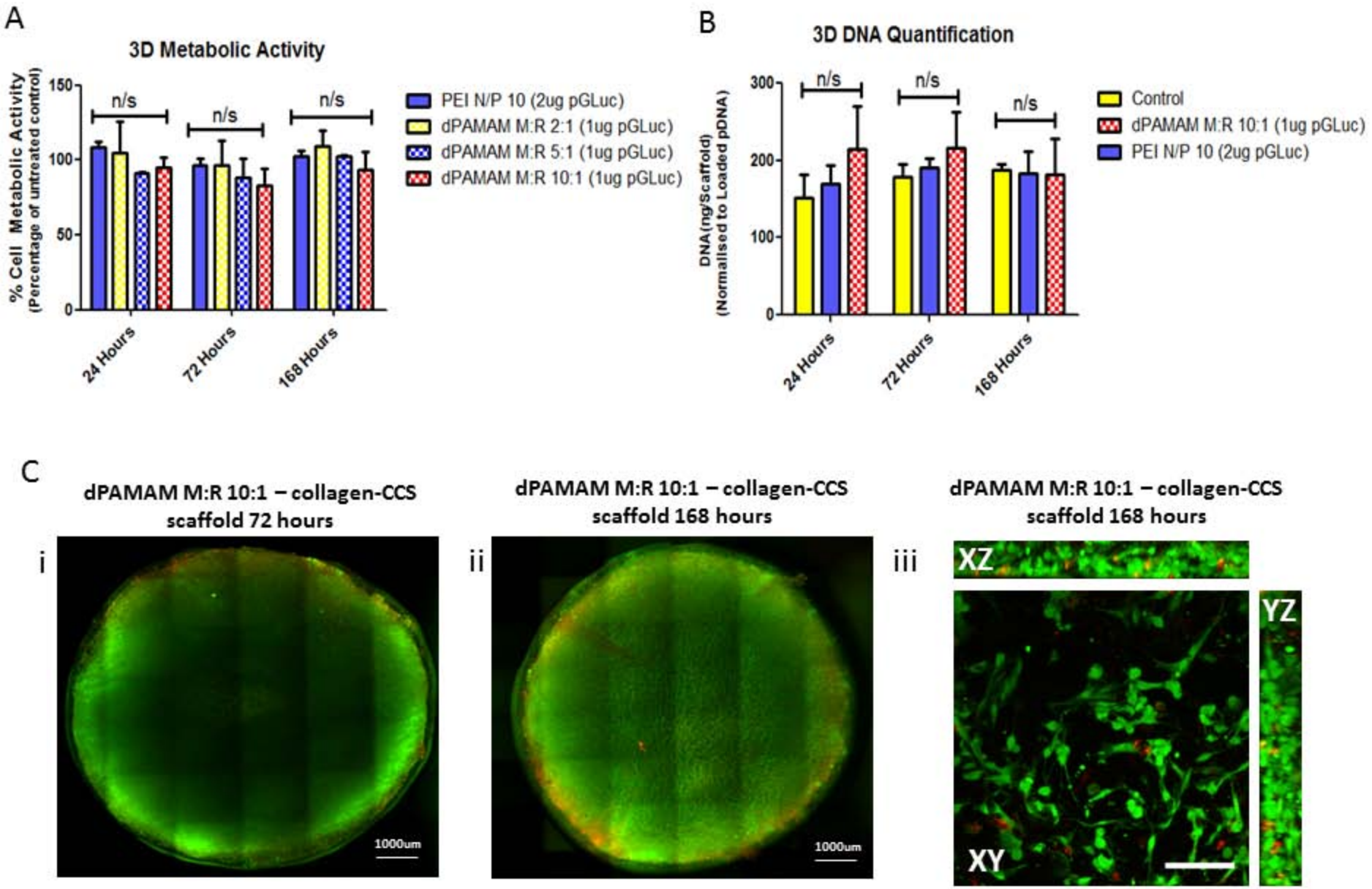
© 2017 Macmillan Publishers Limited. All rights reserved.

Figure 5:



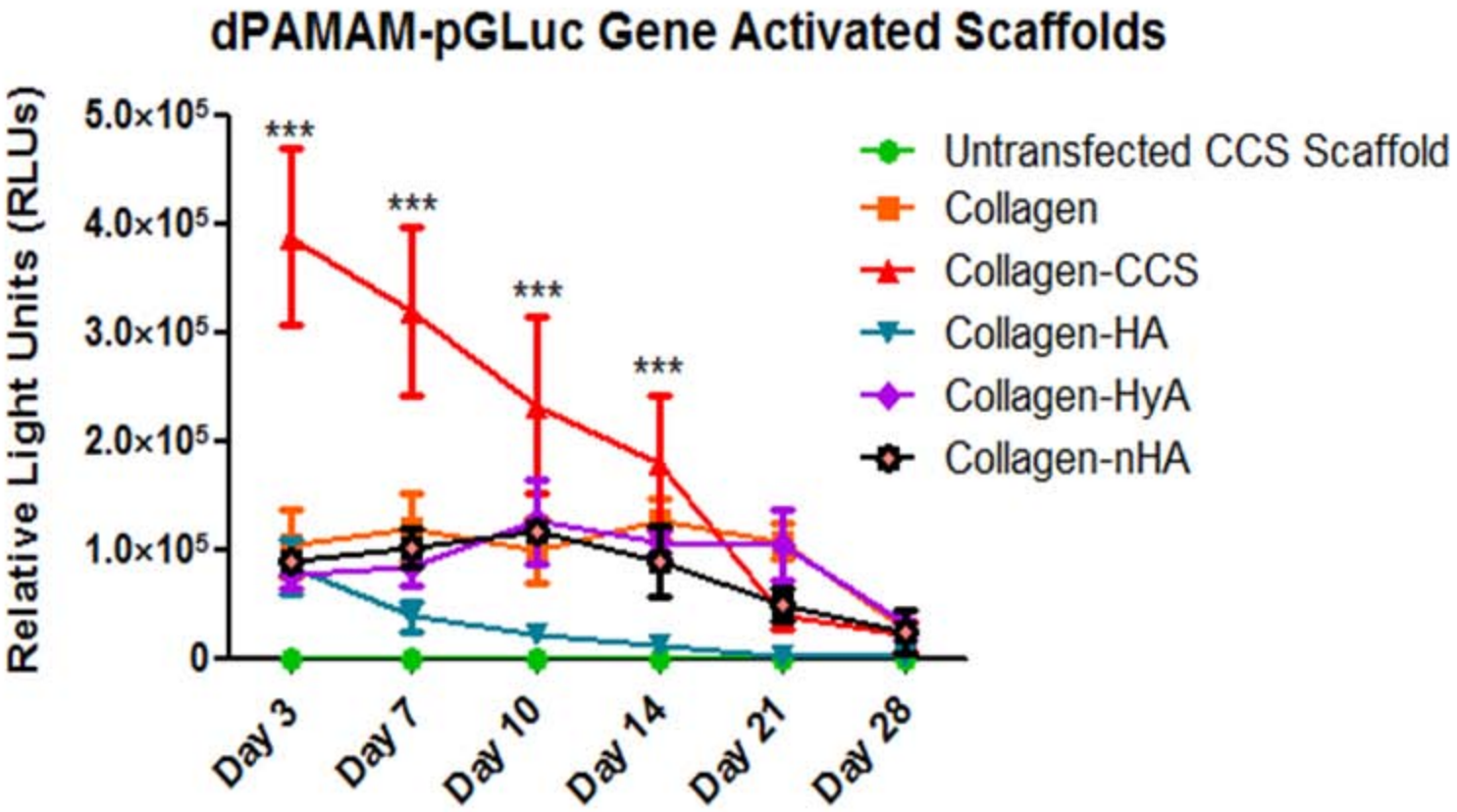
© 2017 Macmillan Publishers Limited. All rights reserved.

Figure 6:



© 2017 Macmillan Publishers Limited. All rights reserved.

Figure 7:



© 2017 Macmillan Publishers Limited. All rights reserved.